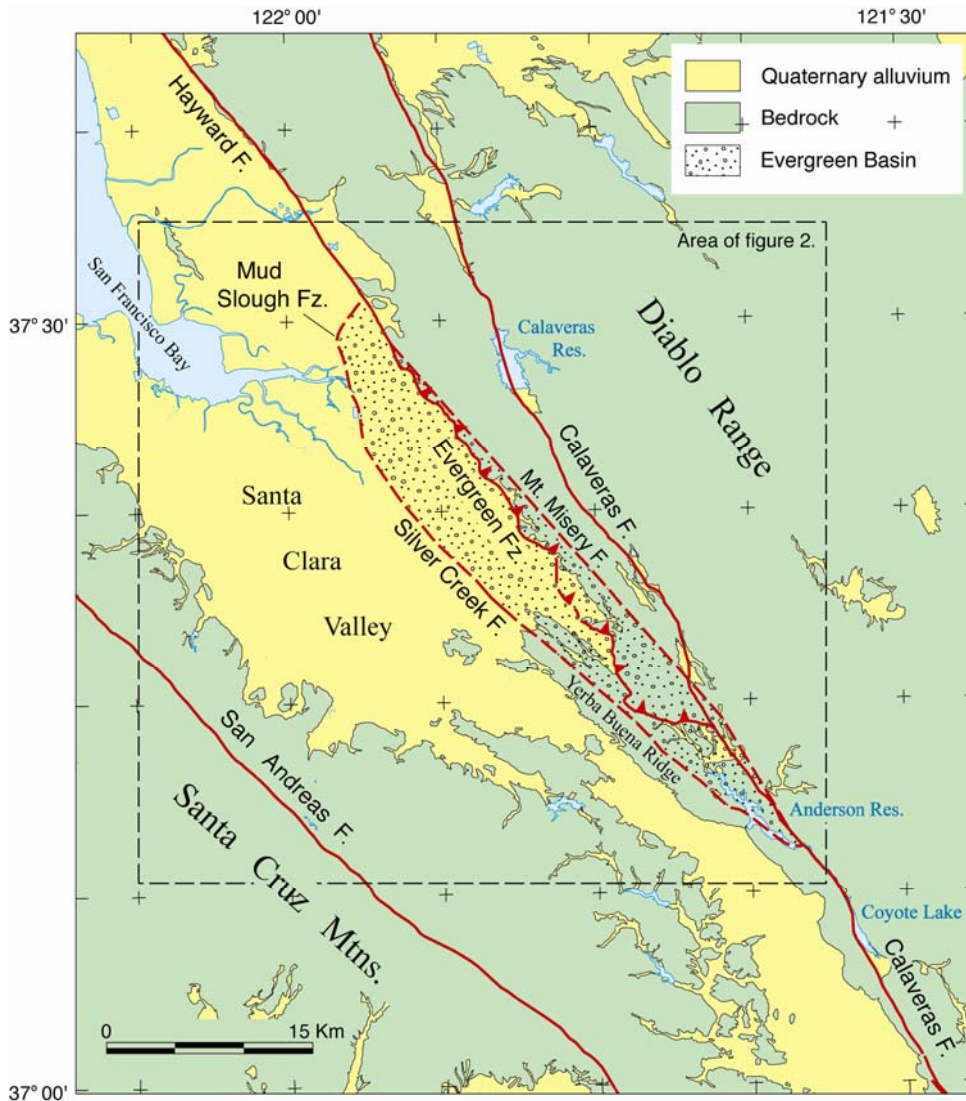# The Quaternary Silver Creek Fault Beneath the Santa Clara Valley, California

By Carl M. Wentworth, Robert A. Williams, Robert C. Jachens, Russell W. Graymer, and William J. Stephenson

Open-File Report 2010-1010

U.S. Department of the Interior
U.S. Geological Survey

U.S. Department of the Interior
KEN SALAZAR, Secretary

U.S. Geological Survey
Marcia K. McNutt, Director

U.S. Geological Survey, Reston, Virginia 2010

The Quaternary Silver Creek Fault Beneath the Santa Clara Valley, California

By Carl M. Wentworth, Robert A. Williams, Robert C. Jachens,
Russell W. Graymer, and William J. Stephenson

Abstract

The northwest-trending Silver Creek Fault is a 40-km-long strike-slip fault in the eastern Santa Clara Valley, California, that has exhibited different behaviors within a changing San Andreas Fault system over the past 10-15 Ma. Quaternary alluvium several hundred meters thick that buries the northern half of the Silver Creek Fault, and that has been sampled by drilling and imaged in a detailed seismic reflection profile, provides a record of the Quaternary history of the fault. We assemble evidence from areal geology, stratigraphy, paleomagnetics, ground-water hydrology, potential-field geophysics, and reflection and earthquake seismology to determine the long history of the fault in order to evaluate its current behavior.

The fault formed in the Miocene more than 100 km to the southeast, as the southwestern fault in a 5-km-wide right step to the Hayward Fault, within which the 40-km-long Evergreen pull-apart basin formed. Later, this basin was obliquely cut by the newly recognized Mt. Misery Fault to form a more direct connection to the Hayward Fault, although continued growth of the basin was sufficient to accommodate at least some late Pliocene alluvium. Large offset along the San Andreas-Calaveras-Mt Misery-Hayward Faults carried the basin northwestward almost to its present position when, about 2 Ma, the fault system was reorganized. This led to near abandonment of the faults bounding the pull-apart basin in favor of right slip extending the Calaveras Fault farther north before stepping west to the Hayward Fault, as it does today. Despite these changes, the Silver Creek Fault experienced a further 200 m of dip slip in the early Quaternary, from which we infer an associated 1.6 km or so of right slip, based on the ratio of the 40-km length of the strike-slip fault to a 5-km depth of the Evergreen Basin. This dip slip ends at a mid-Quaternary unconformity, above which the upper 300 m of alluvial cover exhibits a structural sag at the fault that we interpret as a negative flower structure. This structure implies some continuing strike slip on the Silver Creek Fault in the late Quaternary as well, with a transtensional component but no dip slip.

Our only basis for estimating the rate of this later Quaternary strike slip on the Silver Creek Fault is to assume continuation of the inferred early Quaternary rate of less than 2 mm/yr. Faulting evident in a detailed seismic reflection profile across the Silver Creek Fault extends up to the limit of data at a depth of 50 m and age of about 140 ka, and the course of Coyote Creek suggests Holocene capture in a structural

depression along the fault. No surface trace is evident on the alluvial plain, however, and convincing evidence of Holocene offset is lacking. Few instrumentally recorded earthquakes are located near the fault, and those that are near its southern end represent cross-fault shortening, not strike slip. The fault might have been responsible, however, for two poorly located moderate earthquakes that occurred in the area in 1903. Its southeastern end does mark an abrupt change in the pattern of abundant instrumentally recorded earthquakes along the Calaveras Fault—in both its strike and in the depth distribution of hypocenters—that could indicate continuing influence by the Silver Creek Fault. In the absence of convincing evidence to the contrary, and as a conservative estimate, we presume that the Silver Creek Fault has continued its strike-slip movement through the Holocene, but at a very slow rate. Such a slow rate would, at most, yield very infrequent damaging earthquakes. If the 1903 earthquakes did, in fact, occur on the Silver Creek Fault, they would have greatly reduced the short-term future potential for large earthquakes on the fault.

Introduction

A basement-bounding fault beneath the eastern Santa Clara Valley that we call the Silver Creek Fault has gradually taken on an uncertain importance since it was first proposed in the 1950s. Taylor (1956) delineated such a fault from gravity evidence in 1956 as a northwest-trending fault beneath the eastern Santa Clara Valley (fig. 1), where it is concealed beneath Quaternary alluvium. Earlier, in 1951, Crittenden had described an aligned, northwest-trending thrust fault from bedrock exposures to the southeast along Silver Creek on Yerba Buena Ridge that he also called Silver Creek (fig. 2). Contrasting geologic relations of the two presumed parts of the same structure have proved confusing, and the potential of this structure for generating earthquakes has been uncertain. We now consider these to be two separate faults with very different histories, a relatively superficial thrust and a long, deeply penetrating strike-slip fault. The latter is the subject of this paper. Our goal is to evaluate the Quaternary behavior of the fault, but to do this we need to establish its longer history within the San Andreas Fault System as a basis for forward extrapolation.

We assemble here a summary of what we know about the Silver Creek Fault from our study of the area during the past 15 years, both in its pre-Quaternary participation in the San Andreas fault system in the Bay region and its less clear behavior as a Quaternary fault after major reorganization of the East Bay part of that fault system. Its pre-Quaternary role was as the western of a right-stepping pair of faults between which a 40-km-long pull-apart basin formed—the Evergreen Basin. This role persisted after the basin was obliquely cut by an inferred fault that we call the Mt. Misery Fault. That fault provided a more direct connection to the Hayward fault and subsequently accommodated more than 100 km of right slip running up the East Bay fault system. The Quaternary reorganization saw both of these basin-bounding faults abandoned in favor of slip running up the central Calaveras Fault and thence stepping left onto the Hayward Fault farther north, as it does now. The issue,

2

for the Silver Creek Fault, is to determine whether this abandonment was complete, and if not, in what fashion and at what rate the fault is still moving.

Our basic logic is to establish the presence of the Silver Creek Fault as a basement fault and then to trace its history forward in geologic time. This approach addresses its size and style, its role in the tectonic regime, and any changes that may have occurred in its behavior through time. Confidence in understanding a late Cenozoic fault comes from a well-established geologic history, including bedrock offset and Quaternary history, and then demonstrable evidence of any recent movement.

We draw on a wide range of studies that bear on defining the Silver Creek Fault and its geologic history within the late Cenozoic San Andreas Fault system. We first summarize its geologic setting, particularly its place in the San Andreas Fault system and the sedimentary stratigraphy that lies across and adjacent to the fault, and discuss the age constraints on the timing of identifiable geologic events in its history. Then, in the following sections, we develop relevant topics in more detail. We address fault nomenclature and the history of map representations, because there are opportunities for confusion and error in the literature. After describing how we depict the Silver Creek Fault, we summarize its pre-Quaternary history and assemble evidence that bears on its Quaternary history. As it turns out, a large, strike-slip Silver Creek Fault was established in pre-Quaternary time, but its structural context and behavior changed in the Quaternary, and its recent behavior is not clear.

Geologic Setting

The Santa Clara Valley lies within the San Andreas Fault system between the San Andreas and Calaveras Faults in the southern San Francisco Bay region (figs. 1 and 2; and see fig. 8). It is floored by about 300-500 m of flat-lying Quaternary sediment of the Santa Clara Basin that accumulated as the valley gradually subsided (Wentworth and others, 2005). Unconformably concealed beneath that section is a central basement high of Franciscan assemblage and Coast Range ophiolite and flanking sedimentary basins (figs. 2 and 3). The deep Evergreen Basin, on the east, is separated from the central basement high by the steeply-dipping Silver Creek Fault, which was an important strike-slip participant in the San Andreas system prior to about 2 million years ago (Ma) (Jachens and others, 2002; Jachens and others, 2005; Graymer and others, 2005). The very different Cupertino Basin, on the west, deepens gradually westward and contains oil-bearing marine Miocene sedimentary rocks (Stanley and others, 2002). Another concealed structure that bears indirectly on the Silver Creek Fault is the San Leandro synform, which is located to the northwest beneath San Francisco Bay (fig. 8). Like the Cupertino Basin, this synform contains gently inclined layers that are unconformably truncated by flat-lying deposits (Marlow and others, 1999).

Structure beneath the eastern part of the Santa Clara Valley is well imaged by the Evergreen seismic reflection profile of Williams and others (2002; fig. 4), which shows a subhorizontally layered Quaternary section overlying a prominent reflection at the top of the central basement high. That reflection terminates eastward at the Silver Creek Fault, beyond which the largely flat-lying sedimentary fill within the Evergreen Basin is imaged down beneath the level of the adjacent basement surface to a depth of at least about 1.2 km.

The principal evidence for the shapes and extents of these buried basins comes from detailed gravity measurements and their interpretation (figs. 5 and 8). The lower density of the sediment and rock filling the basins, compared with that of adjacent basement rock, produces distinct gravity lows. This strong density contrast provides the basis for applying an iterative, direct inversion procedure that partitions the gravity signal into one component that reflects the density distribution in the basement and another that reflects the low-density basin fill (Jachens and Moring, 1990). This latter component is then converted to a thickness of fill based on a function of density versus depth within the basin. The results of such basin-fill inversions for the aforementioned basins are shown in figures 5 and 8 (as elevation relative to sea level). The Evergreen Basin is revealed as a steep-sided structural depression several kilometers deep that trends northwest for about 40 km from the Calaveras Fault at the southeastern end of Anderson Lake (Jachens and others, 2002). The accuracy of such basin inversions is critically dependent on knowledge of the variation of density versus depth in the basin fill, for which we have very limited direct information. The more general density information used for the inversions presented here yields basins whose relative shapes are correct but whose absolute depths are less certain.

The actual depth to the base of the sedimentary fill in the Evergreen Basin is probably about 5 km, but could be somewhat deeper. The gravity inversion yields maximum depths of about 4.5 to 5.5 km and about 4 km at the cross section of figure 3. Velocity modeling from earthquake data by Michael (1988) suggests a depth of more than 5 km. We use 5 km as a reasonable approximation.

The Quaternary alluvial fill of the Santa Clara Valley (the Santa Clara Basin; fig. 6) is underlain by an unconformity that extends across the whole Santa Clara Valley, lies directly on the mid-basin basement high, truncates late Miocene sedimentary rocks of the Cupertino Basin on the west, and crosses Pliocene Evergreen Basin fill on the east (fig. 3). Distinctive Plio-Pleistocene gravels are exposed on both sides of the valley, but the centrally located well GUAD, which penetrated the alluvial section and reached the underlying Franciscan basement at a depth of 1,336 ft (407 m), encountered none of these gravels (figs. 2 and 6; Andersen and others, 2005). Either the gravels were never deposited within the valley because the basement was too high or they were subsequently removed by erosion (Jachens and others, 2005). Most of these gravels are considered to range in age from Pliocene up into the early Pleistocene, which places the unconformity in the early Pleistocene. The episode of erosion that produced this basal unconformity may well have been a

product of events related to the 2-Ma reorganization of the East Bay fault system (see Pre-Quaternary Silver Creek Fault).

Subsequently, the whole Santa Clara Basin began to subside and accumulate alluvial sediment. The resultant Quaternary section consists of an upper 1,000 ft or so (300 m) of relatively coarse alluvium and a lower fine-grained section about 350-500 ft (100-150 m) thick (fig. 6). Study of several research drill holes (Newhouse and others, 2004), together with selected drillers logs of water wells (Leighton and others, 1995), have permitted a fairly detailed understanding of this Quaternary section (Wentworth and Tinsley, 2005a and 2005b; Wentworth and others, 2005).

Wentworth and Tinsley (2005a, b) have subdivided the coarser, upper part of the Quaternary section into eight upward-fining alluvial sequences that can be correlated with the major climate-driven oscillations evident in the marine oxygen isotope record. No age-diagnostic fossils have been recovered from these deposits, but the correlation with the dated marine isotope record provides a means of estimating the age of each of the sequences. The base of cycle 8 is thus about 750 ka, which is consistent with the presence of a paleomagnetic reversal just 22 ft (6.7 m) deeper in well CCOC that Mankinen and Wentworth (2003) can correlate with the 780-ka Bruhnes/Matuyama paleomagnetic boundary. Cycle 1 is largely Holocene (0-11.8 ka), although accumulation of this latest alluvial cycle actually began somewhat earlier (Wentworth and Tinsley, 2005a, b). These eight sequences record a very regular subsidence of the Santa Clara Basin at a rate of 0.38 mm/yr during the past 750,000 yrs relative to high-stand sea level (like that of today).

The lower, fine-grained section also appears to be nonmarine, inasmuch as careful examination of drill cuttings from GUAD has revealed no microfossils and a core taken near the base of the section is poorly sorted and apparently alluvial. An unconformity at the top of this lower section in the deep drill hole MOFT, near San Francisco Bay (fig. 2), is indicated by an abrupt downward increase in density just below the base of cycle 8 (fig. 6). We place this horizon at an equivalent position in GUAD within an interval of reversed paleomagnetic polarity that seems much too thin (38 ft; 11.6 m) to represent the 210,000-yr-long Matuyama polarity epoch (E.A. Mankinen and C.M. Wentworth, unpublished data). We generalize the age of this upper unconformity to be about 975 ka, and that at the base of the fine-grained section to be about 1.5 Ma, through downward extrapolation of the sedimentation rate for the overlying section (see Timing and Ages, below).

The Evergreen Basin is presumably filled with Miocene and Pliocene sedimentary deposits (see Pre-Quaternary Silver Creek Fault), of which only the Pliocene Silver Creek gravels are exposed. A 2.6-Ma basalt dates the exposed upper part of these gravels (Nakata and others, 1993; Wentworth and others, 1998). After deposition of the Silver Creek gravels, a fundamental reorganization of the East Bay fault system occurred (see Pre-Quaternary Silver Creek Fault) that transferred principal slip from the faults bounding the Evergreen Basin to a new, northerly segment of the Calaveras Fault, creating a left step from there onto the Hayward

Fault. Subsequent thrusting related to this Quaternary left step has driven Mesozoic rocks of the Great Valley sequence entirely across the central part of the basin to form a thrust flap (F in fig. 2) that reaches Yerba Buena Ridge. The locally derived Packwood gravels, which overlap some of the thrusts (Crittenden, 1951; Wentworth and others, 1998), are largely to completely younger than the Silver Creek gravels and range up into the early Pleistocene (Graymer and others, 2005; Jachens and others, 2005).

Shallow, cross-fault shortening is common along the southern part of the Silver Creek Fault, including a thrust named Silver Creek (see Past Representations of the Silver Creek Fault), and such shortening extends along much of the east side of the Evergreen Basin (fig. 2). It is not clear the extent to which any shallow or exposed remnants of the strike-slip Silver Creek Fault remain along Yerba Buena Ridge that are not modified by this thrusting.

Timing and Ages

We cannot be precise in specifying the timing of the various geologic events related to the Silver Creek Fault, because they cannot be directly dated. The constraints on the timing of the reorganization of the East Bay strike-slip system are rather broad, between the 2.6-Ma age of the basalt interbedded in the upper Silver Creek Gravels and the early Quaternary age of younger Packwood gravels (somewhat after the 1.8 Ma beginning of the Quaternary Period). For simplicity in discussion we take the age of reorganization to be about 2 Ma.

We note that the definition of the Quaternary Period has recently been changed to extend its beginning from 1.8 back to 2.6 Ma (Mascarelli, 2009; Walker and Geissman, 2009). Because this paper has been prepared in the context of the old definition, as was all the work on which it is based, we have retained the earlier definitions of Pliocene, Pleistocene, and Quaternary. This difference has no bearing on our use of 1.8 Ma, as the redefinition of the Quaternary in no way changes the age significance of the evidence on which we base our age assignments.

The age of the basin-wide unconformity at the base of the Quaternary section (figs. 3 and 6) is bracketed between the Plio-Pleistocene age of the Santa Clara and other gravels and the age of the base of that Quaternary alluvial section. We have noted that the gravels are not present above Franciscan basement in GUAD, which means either their non-deposition or erosion prior to accumulation of the Quaternary section. The age of the base of that section, in turn, depends on an uncertain estimate of the time represented by the lower fine-grained section. For that estimate, we assume that the 0.38 mm/yr subsidence rate for the upper Quaternary section can be applied to the underlying 350-500 ft (100-150 m) of fine grained section, which yields a time interval of about 300-400 ka. Adding that to the 990-ka age of the base of the Matuyama reversed polarity epoch places the base of the fine-grained section at about 1.3-1.4 Ma. We then take the age of the unconformity to be about 1.5 Ma.

The age of the mid-Quaternary unconformity within the Matuyama polarity epoch is bracketed by the age range of that interval, 780-990 ka. Again assuming that the 0.38 mm/yr rate can be applied here, the 38-ft section would represent about 30,000 yrs, the hiatus would be about 180,000 yrs long, and placing the unconformity in the middle of the reversed section at the beginning of the hiatus makes it about 975 ka.

There is much emphasis in seismologic and engineering geologic practice on activity within Holocene time (0-11.8 ka) in determining whether a fault has moved recently enough to be of practical concern as an active fault. Sedimentary cycle 1 is our best approximation of that time interval in the stratigraphy we describe. Cycle 1 is largely Holocene, but its base is somewhat older, as this cycle began accumulating after the 18-ka age of the just-preceding glacial maximum and before a 12.4-ka carbon-14 age located just above a basal, 15-ft-thick sand and gravel (4.6 m; Wentworth and Tinsley 2005a, b).

Past Map Representations of the Silver Creek Fault

There are two faults named Silver Creek in the Santa Clara Valley that must be distinguished. One is the long, steep, basement-cutting Silver Creek fault that bounds the west margin of the Evergreen Basin, but there is also a Silver Creek Fault zone defined by Crittenden (1951) from exposures on Yerba Buena Ridge that includes a west-dipping thrust (and see Wentworth and others, 1998). We use Silver Creek Thrust to designate this thrust fault, and Silver Creek Fault for the basement-bounding fault that is the subject of this report.

Map depiction of the Silver Creek Fault beneath the alluvial plain in the Santa Clara Valley has differed over the years. The earliest we have found is that of Taylor (1956), in which he used gravity to map a Silver Creek Fault emanating from the mouth of Silver Creek and then splitting into two subparallel branches about 2.9 km apart, both of which pass east of Coyote Hills. Jennings and Burnett used Taylor's fault traces in their 1961 geologic compilation of the 1:250,000-scale San Francisco sheet of the Geologic Map of California (Jennings and Burnett, 1961).

A geologic map was published in 1967 as part of Appendix A to Bulletin 118 (Plate 3, California Department of Water Resources, 1967) that shows a single Silver Creek Fault trace extending northwest from Yerba Buena Ridge and passing east of Coyote Hills. A second fault is shown splaying northward from the Silver Creek Fault east of the southern end of San Francisco Bay.

The source of these fault traces is revealed in an annotated manuscript version of an identical map found by G.J. Saucedo in the files of the California Geological Survey. This map indicates that the fault traces and the basement surface contours in Plate 3 were "inferred from gravity data" by Roger Chapman, who was a geophysicist with the then named California Division of Mines and Geology (now California Geological Survey). It is this version of the Silver Creek Fault that T.H. Rogers used

in his compilation of the 1:250,000-scale San Jose Sheet of the Geologic Map of California (Rogers, 1966).

A very different fault pattern is shown in the groundwater report (California Department of Water Resources, 1975) for which the 1967 report is Appendix A. Here a maze of variously trending faults is shown in the Santa Clara Valley based on truncations of presumed narrow alluvial channel sands inferred from drillers logs of water wells. In this rendition, the Silver Creek Fault is extended on strike for about 5.6 km northwest from Yerba Buena Ridge, where it is truncated by a supposed north-trending fault named the Edenvale Fault.

The principal source for the past map depictions of faults concealed beneath the Santa Clara Valley, including the Silver Creek Fault, seem ultimately to be these two different parts of Bulletin 118 of the California Department of Water Resources, one based on gravity, the other on truncations of inferred channels. Pampeyan (1979) uses them, Wagner and others (1991) use Pampeyan, and Jennings and Saucedo (1994) use Wagner and others, as well as the two parts of Bulletin 118.

A further, different set of faults is inferred by Brabb and Hanna (1981) from magnetic anomalies produced largely by serpentinite in the basement beneath the Santa Clara Valley. Serpentinites typically can be used to help delineate faults in Franciscan terrane, but these old structures have not necessarily experienced any late Cenozoic movement at all.

We do not consider the faults based on truncations of inferred stream channels (fig. 5 of California Department of Water Resources, 1975) to be reasonable, either in the channel interpretation or in the resultant fault pattern. The channel interpretation involved arbitrary subdivision of the Quaternary section into 50-ft-thick intervals and the assumption that narrow sand channels had been preserved within those 50-ft intervals (15 m thick). Our sequence stratigraphic analysis yields a very different subdivision of the water-bearing alluvial section, namely eight generally upward-fining sequences with an average thickness of 120 ft (36 m). Instead of consisting of isolated sand channels, the coarse bases of these sequences are more or less laterally continuous, as they can be mapped across much of the valley in wells. And, inasmuch as the Chapman set of faults is based solely on gravity, we can reevaluate those faults based on modern gravity data and methods. In effect, then, we must start over in determining the presence of any late Cenozoic faults concealed beneath Santa Clara Valley. Any continued dependence on the Department of Water Resources maps or their derivatives is now without foundation. Here, we focus on what we can say about the Silver Creek Fault using modern data and techniques.

Present Delineation

We delineate the Silver Creek Fault as the western basement boundary of the Evergreen Basin in the fashion begun by Taylor (1956) and Chapman (California Department of Water Resources, 1967, Plate 3), but using the current array of gravity

stations and the basin-thickness inversion of gravity (fig. 5), which sharpens the gravity depiction of the basin boundaries. The western boundary of the basin is relatively straight, and the principal issue in locating the fault is just how high on the steeply east-dipping basin boundary in the gravity inversion to place the bedrock trace.

There is no convincing evidence for the location of the fault on the alluvial surface (see Quaternary Behavior), but two independent lines of evidence indicate that the trace lies at the top of the gravity boundary. A steep gradient in an InSAR image (Ikehara and others, 1998; Galloway and others, 1999 and 2000; fig. 15) marks an abrupt subsidence boundary with as much as 2.5 cm of recoverable annual subsidence west of the Silver Creek Fault that results from groundwater pumping. This subsidence boundary requires a groundwater boundary in the water-bearing section, which we take to mark the shallow expression of the Silver Creek Fault (and see Quaternary Behavior of the Silver Creek Fault). Independent confirmation of a basement-bounding Silver Creek Fault and its location is provided by the Evergreen seismic reflection profile (fig. 4). The eastward termination of the basement reflection at the Silver Creek Fault in that profile occurs directly beneath the location of the InSAR boundary. We thus place the bedrock trace of the Silver Creek Fault along the top of the basin boundary in the gravity inversion, extending northwestward from its intersection with the Calaveras Fault.

The northwest end of the basin is marked by a gentle, east-to-southeast-facing gravity gradient extending to the Hayward Fault that presumably consists of a set of normal faults stepping down into the basin (Chapman's north-trending fault splay reflected this same gradient). We represent this fault zone as a single map trace that trends north and northeastward from the Silver Creek Fault across largely undeveloped mud flats, and name it the Mud Slough Fault zone for a slough of that name at the southeastern end of San Francisco Bay.

The Silver Creek Fault thus defined is not coincident with faults at the surface for much of its length beneath Yerba Buena Ridge. This emphasizes the fact that the structure exposed on the ridge is above the main basement boundary and reflects the cross-fault shortening associated with the thrust flap of Mesozoic rocks, including the Silver Creek Thrust.

Pre-Quaternary Silver Creek Fault

The San Andreas Fault has undergone about 300 km of right slip along its central, unbranched section (Ross, 1970; Mathews, 1976). In the San Francisco Bay region, 175 km of this slip branches eastward onto the southern Calaveras fault and thence northwest to other East Bay faults (McLaughlin and others, 1996; Graymer and others, 2002). These offsets are determined from correlations between rocks on either side of the various faults. The large body of serpentinite exposed on Yerba Buena Ridge and in the subsurface to the northwest (fig. 2) has no nearby equivalent

east of the Evergreen Basin. In fact, no equivalent rocks are found to the southeast short of the Parkfield area, where a correlative body of serpentinite indicates that the Yerba Buena rocks represent the full 175 km of East Bay offset (Jachens and others, 2002). This offset involves both large right slip on the central San Andreas and southern Calaveras Faults and 40 km of slip on the Silver Creek Fault itself.

The strike slip on the Silver Creek Fault initially stepped right onto an early version of the Hayward fault (fig. 7A). Extension at this right step led to the gradual opening of a large pull-apart basin east of the Silver Creek Fault that became the 40-km-long Evergreen Basin (Jachens and others, 2002). As the basin opened, it presumably accumulated Miocene and perhaps Pliocene sedimentary fill that is now concealed beneath the Plio-Pleistocene gravels exposed on the east side of Yerba Buena Ridge and south of the Mesozoic thrust flap that covers the central part of the basin. Continuity of the basin fill beneath this thrust flap is supported both by continuity of the gravity low and low seismic P-wave velocities (Michael, 1988).

Once the basin was well developed, we infer, right slip broke obliquely across the basin to more directly connect the Calaveras to the Hayward Fault (fig. 7B). Evidence for this is the southward narrowing of the present basin and its straight eastern side, nicely aligned to define that crosscutting connection (figs. 5 and 7B). We envision this history to be similar to that developed by Anderson and others (2004) for the San Bernardino graben, although that graben has yet to have its two parts completely separated by continuing slip on its crosscutting San Jacinto fault. We name the fault that crosscut the Evergreen Basin the Mt. Misery Fault (fig. 1), for a mountain located near its southern end. Today the Mt. Misery Fault is everywhere concealed beneath the Evergreen Thrust system at the east side of the Evergreen Basin.

This newly formed Mt. Misery Fault was positioned to carry much of the large right slip from the Calaveras north to the Hayward Fault, thus accounting for more than 100 km of the offset between Parkfield and the Yerba Buena rocks. Candidates for the eastern, offset part of the Evergreen Basin exist in about the right location down the San Andreas Fault, but exploration of that topic is beyond the scope of this paper. Following the formation of the Mt. Misery Fault, the Silver Creek Fault must have absorbed some additional right slip, or at least some further down-to-the-east movement, for the Evergreen Basin contains late Pliocene sediment (Silver Creek gravels).

The fact that strike-slip motion on the southern Calaveras Fault now proceeds up the central Calaveras Fault to Calaveras Reservoir, bypassing both the Silver Creek and Mt. Misery Faults, indicates a major reorganization of the East Bay fault system (fig. 7 C). Calaveras offset of the Franciscan boundary at San Felipe Valley is only 2-3 km (fig. 8; Wentworth and others, 1998), so this present deformation pattern cannot be very old. Details of the surface geology along the northeast side of Yerba Buena Ridge show that the youngest basin fill is as young as Pliocene (2.6 Ma) and that the oldest thrusts associated with post-reorganization deformation (see

Quaternary Behavior) are overlain by early Pleistocene Packwood gravels (Wentworth and others, 1998; Graymer and others, 2005). This indicates that prominent strike slip on the Silver Creek and Mt. Misery Faults terminated about 2 Ma, which dates the reorganization of the fault system from the Evergreen Basin to central Calaveras slip (and see Timing and Ages, in Geologic Setting).

Possible Northwestward Extension

Although we have closed the northwest end of the pull-apart basin against the Hayward Fault along the Mud Slough Fault zone in accordance with the gravity gradient, the Silver Creek Fault might also continue northwestward on strike past the Coyote Hills. Both Taylor (1956) and Chapman (California Department of Water Resources, 1967) carried a Silver Creek Fault northwestward along the east side of the Coyote Hills, and Catchings and others (2006) suggest that the fault extends more than 35 km northwestward across the western part of their San Leandro seismic profile (see fig. 8). The very presence of the northwest-trending Coyote Hills on an otherwise flat Bay plain attracts such an interpretation.

A northwest extension of the Silver Creek Fault should be a late Cenozoic, right-lateral strike-slip fault, given its on-strike continuation from the Silver Creek Fault and a trend parallel to the San Andreas and Hayward Faults. It would be a long fault, and would be favorably positioned to have absorbed a considerable part of the large East Bay component of right slip in the San Andreas system.

Geologic evidence for such a fault could involve offset of distinctive rocks in the Franciscan basement, preservation of buried late Tertiary rocks against a basement fault, or offset of the basement surface beneath its present Quaternary cover. Negative evidence, in addition to the absence of these features, could involve crosscutting features that are not offset.

Basement structure in the vicinity of the Coyote Hills does trend northwestward, as expressed in the Franciscan rocks exposed in the hills (Snetsinger, 1976) and in magnetic lineaments arising from elongate bodies of magnetic basement rock (fig. 8; Roberts and Jachens, 2003). These magnetic rocks are presumed to be largely serpentinite, but at least in the Coyote Hills they involve Franciscan greenstone as well. Testing of rocks with a magnetic susceptibility meter by Jachens on a foot traverse around the perimeter of the hills demonstrated that greenstone along the west side of the hills is magnetic, whereas that along the east side is not, indicating that this contrast in greenstone susceptibility at least locally defines the eastern boundary of the magnetic body aligned along the Coyote Hills.

Farther northwest, the west side of a magnetic body beneath the eastern San Leandro synform is imperfectly aligned with the east side of the Coyote Hills body (fig. 8). Truncation beneath that synform of the eastern end of a more westerly

11

trending magnetic body indicates structural discontinuity there, at least in the Mesozoic basement rocks.

It is tempting to postulate an extension of the Silver Creek Fault that follows the eastern side of the Coyote Hills magnetic body and then the western, discordant side of the more northwesterly body. But there are problems, of which the imperfect alignment of the two magnetic lineaments is the least. The east side of the Coyote Hills body actually passes over the northern part of Franciscan basement exposed in the hills with no indication of late Cenozoic movement. Greater constraint for this or any similar alignment is imposed by the southern boundary of the San Leandro synform (fig. 8; Marlow and others, 1999), which shows no evidence of significant fault offset. Finally, any large fault on this trajectory would encounter the cross-trending Mesozoic Novato Quarry terrane farther northwest (Graymer and others, 2002), the continuity of which denies large strike-slip offset (fig. 8). Closing a Silver Creek extension northward against the Hayward Fault to avoid the Novato Quarry terrane would create a releasing bend in the strike-slip system that should be marked by a structural depression that does not exist. An alternative would be to pass a Silver Creek extension along the west side of the Coyote Hills, but this encounters the same problems to the northwest, with the additional constraint of the unbroken magnetic body beneath the center of the San Leandro synform.

More local constraints can be examined through the numerous P-wave seismic refraction profiles collected by Hazelwood (1974 and 1976). Profile A (fig. 8), in the southeastern corner of the San Leandro synform, as well as several other profiles farther north (not illustrated), encountered a three-fold stratigraphy: an upper layer of sediment with a seismic velocity of 5,500 ft/s (1.7 km/s), an intermediate layer with a velocity of 7,000 ft/s (2.1 km/s), and a lower layer with an average velocity of about 12,000 ft/s (3.7 km/s) that is appropriate for shallow Franciscan rock.

We can correlate the upper part of the Quaternary alluvial section in the Santa Clara Valley northeastward across the Coyote Hills (fig. 9), and then extend that correlation to Hazelwood's upper refraction layer. His bottom refraction layer is Franciscan basement. We suggest that the intervening layer is the fill of the San Leandro synform, presumably Tertiary, which was imaged beneath an angular unconformity by Marlow and others (1999). For comparison, the P-wave velocity of the upper 38 ft (11.6 m) of Miocene sandstone beneath Quaternary cover in the Cupertino Basin, measured by suspension velocity logger in research drill hole MGCY (fig. 2), is also about 2.1 km/s (see Newhouse and others, 2004). The intermediate layer is missing south of profile A in all the profiles around the Coyote Hills (fig. 8), where the Quaternary section thus lies directly on Franciscan basement.

The buried surface of Franciscan basement around the Coyote Hills shows no good evidence of either lateral or vertical offset at the limited resolution of the data (fig. 8). The basin-thickness inversion of gravity shows a rather simple, relatively flat surface between the San Leandro and Evergreen Basins, interrupted only by the Coyote Hills ridge. Gridding of elevations from several drill holes to basement and

from migrated depth points reported by Hazelwood yields a more intricate bedrock surface that also shows no good evidence of either lateral or vertical offset (fig. 8, inset).

The refraction profiles themselves (fig. 10) provide more detailed representations of the basement surface that also show no clear evidence of vertical fault separation within the resolution of the data. That resolution is implied by the local irregularity of less than 50 ft (15 m) in depth points and separation between results from right- and left-directed shots. In aggregate, the profiles show a relatively smooth and regular basement surface that rises toward the crest of the Coyote Hills ridge. In four places west of the Coyote Hills, on profiles D and E, the right- and left-directed depth points locally separate vertically by as much as about 150 ft (45 m), but smooth basement surfaces can be carried across without evident vertical separation. An apparent vertical separation of about 100 ft (30 m) does occur in profile A across a 900 ft (280 m) horizontal gap between the ends of right- and left-directed lines of depth points. This could represent a real basement step or topographic irregularity, or simply be an artifact resulting from the opposed shooting directions. In any case, the top of layer two (base of the Quaternary) does not seem to be affected.

A short reflection profile just east of the southern Coyote Hills (GM on fig. 2) images an 1,800 ft (550 m) length of the basement surface (see fig. 13). This profile demonstrates that the basement surface is quite smooth, and within the length of the profile, at least, completely unbroken.

The significance of these local constraints on fault offset from the shape of the basement surface around the Coyote Hills is limited by the relatively young age of that surface and its overlying alluvial deposits. The basement surface was transgressively buried by Quaternary sediment beginning at about 1.5 Ma, the age of the basal Quaternary unconformity (see MOFT, fig. 6), and continuing to about 600 ka, the age of the deposits covering the shallow basement around the hills (fig. 9).

Discontinuity in the groundwater system can mark a fault that offsets the water-bearing deposits, as is the case, for example, along the Hayward Fault where it crosses the head of the Niles alluvial cone east of the Coyote Hills. No such groundwater barrier occurs, however, along a northwest trend aligned with the Coyote Hills. Hydraulic continuity in the uppermost, Newark, aquifer (cycle 2 of fig. 9) is demonstrated by intrusion of salt water eastward for 4-5 miles from San Francisco Bay both north and south of the hills (California Department of Water Resources, 1968). Pump testing demonstrated similar continuity in the next deeper, Centerville, aquifer (cycle 3) just south of the hills (California Department of Water Resources, 1967). This evidence simply indicates the absence of groundwater evidence for a fault, for some hydraulic continuity across a fault is quite possible.

It seems clear that the basement surface around the Coyote Hills is principally or entirely a natural erosional feature now largely immersed in Quaternary alluvium.

We see no evidence for a late Cenozoic fault passing either west or east of the Coyote Hills, and considerable evidence to the contrary. Certainly no large, well-integrated late Cenozoic strike-slip fault occurs here, nor is there need for one. All the large right slip that runs up the southern Calaveras Fault to the southeastern end of the Silver Creek Fault can be accommodated without such a fault, as already discussed.

Quaternary Behavior

The most obvious effect of the 2-Ma reorganization of the strike-slip system was the imposition of a left step from the central Calaveras to the Hayward Fault in place of the earlier right step from the Silver Creek Fault and more direct connection along the Mt. Misery Fault. Earthquakes along the present Calaveras-Hayward transition define a smooth continuous connecting surface at depths greater than about 5 km (Simpson and others, 2004; fig. 17). In the shallow crust, however, the left step produced compression resulting in the thrusting of the Mesozoic structural flap across the Evergreen Basin, as well as thrusting along the east side of Yerba Buena Ridge and farther north in the basin. This thrusting has involved Pleistocene deposits, and possibly Holocene deposits as well (Bryant, 1981; Hitchcock and Brankman (2002).

Surface Faulting

The structural reorganization resulted in principal right slip extending the central Calaveras Fault northward, with the result that there is clear evidence of surface faulting north of its junction with the Silver Creek Fault (Witter and others, 2003). This evidence of Holocene displacement led to designation of this northern reach of the central Calaveras Fault as an Earthquake Fault Zone under the Alquist Priolo Earthquake Fault Zoning Act (Bryant and Hart, 2007; California Division of Mines and Geology, 1982). The Silver Creek Fault, in contrast, does not exhibit clear evidence of topographic or Holocene stratigraphic offset and is no longer zoned by the State (Bryant, 1981; California Division of Mines and Geology, 1982). Fault traces along Yerba Buena Ridge had earlier been zoned by the State because they offset Plio-Pleistocene gravels (Bryant, 1981).

There are some reports that suggest young deformation across the Silver Creek Fault on the alluvial plain northwest of Yerba Buena Ridge, but they are far from conclusive. Bryant (1981) reports that in 1971 R.O. Burford measured as much as 6 inches of apparent right-lateral deformation across a 250-foot length of a fence running northeast across the mouth of Silver Creek, but that there are problems with the integrity of the fence. Bryant also notes a consultant report describing even less confident deformation along a nail line in the asphalt of Aborn Road about 1.2 km farther northwest. Hitchcock and Brankman (2002) argue that geomorphic relations involving an arch in the long profile of Coyote Creek and abrupt downstream transition from terraces to alluviation indicate deformation at the Silver Creek Fault,

although the presence of similar variations at other points along the creek, and not just at the Silver Creek Fault, would seem to suggest a nontectonic cause.

Two distinct topographic steps, each about 2 m high, are evident in a detailed elevation profile that was collected along a shallow reflection line (fig. 12) for precise source and geophone location, using a Trimble GeoXH equipped with a Zephyr external antenna. The topographic steps occur within Holocene levee deposits that are mapped along Coyote Creek (Witter and others, 2006), but face away from the creek at the east side of a broad northwest-trending swale. The eastern of the two steps is caught by 5-foot topographic contours at 1:24,000 (U.S. Geological Survey, San Jose West quadrangle, 1961), which show it to be about 1 mile long with a curved trace, trending north and then northwest. The curved trace suggests a drainage-related origin rather than surface faulting related to the underlying Silver Creek Fault. The steps face the wrong way to be terraces of the present Coyote Creek, but they could be related to overbank floodwaters running down the swale.

Minivibroseis Reflection Profile

The strongest evidence for any continued activity along the northern Silver Creek Fault beneath the alluvial plain is recorded in the Evergreen seismic reflection profile (figs. 4 and 11), which was collected in 2002 by Williams and others (2002) using a minivibroseis source (table 1). Despite difficult urban conditions, involving both noise and varied ground conditions ranging from paved streets to sports fields and railroad beds, the survey yielded reflections from depths of about 50 m to 1.2 km within the Evergreen Basin.

Correlation of the base of the Quaternary section across the Silver Creek Fault defines a vertical separation of 200 m (fig. 11). Within the Evergreen Basin, the progressive downward increase in seismic velocity (interval velocity determined from stacking velocities) is interrupted below 2.1 km/s by an abrupt 33-percent increase at a depth of 700 m. This velocity step indicates an unconformity in the basin fill, and we correlate this with the unconformable base of the Quaternary section above Franciscan basement to the west, where the interval velocity is also 2.1 km/s.

The mid-Quaternary unconformity identified in wells MOFT and GUAD is clearly evident in the reflection profile at the base of the laterally continuous reflections at a depth of about 0.33 km (fig. 11), a position just below the projected bottom of well CCOC, which is where the unconformity should occur (fig. 6). We have correlated the unconformity across the eastern part of the record in figure 11 at about the same position relative to overlying reflections. Below this unconformity the reflections are not continuous across the fault, whereas above they can be traced across with confidence, albeit with some modest deformation. The 200-m step in the basal Quaternary unconformity thus must have developed before the mid-Quaternary unconformity, or during the period of approximately 2 Ma to 975 ka (a duration of about 1 Ma).

15

Accomplishing 200 m of vertical separation on the base of the Quaternary section by slightly oblique strike slip seems reasonable, given the earlier history of the Silver Creek Fault, although it implies considerable right slip in the early Quaternary. Over 1 Ma, that separation represents dip slip of 0.2 mm/yr. Using the proportion of strike to dip slip during growth of the Evergreen Basin of about 40 km to 5 km, or 8:1, this would indicate 1.6 km of right slip over 1 Ma in the early Quaternary, or an average rate of 1.6 mm/yr.

The Silver Creek Fault can be confidently traced upward from the 500-m-deep bedrock tip of the fault to and slightly above the mid-Quaternary unconformity. Above that the deformation is much less distinct, although here also we suggest that the fault has broken the shallow section and offset individual reflections by less than a cycle (red dots in fig. 11). The reflections in the shallow section define a distinct structural sag across the Silver Creek Fault that, near the surface, is about 750 m wide with an amplitude of about 30 m. This amplitude decreases downward, as does the width of the sag, with the sag still distinct as deep as almost 300 m. The sag is evident as shallow as about 50 m, above which no coherent reflections were obtained. The structural sag is marked by numerous steps and bends in the reflections of less than a cycle that imply small faults, with both normal and reverse separations. Although the presence of small faults is clear, delineating their extent in the profile is not, and we have refrained from attempting a more complete fault delineation in figure 11.

These characteristics of the structural sag—an upward spreading synformal structure marked by faults of both normal and reverse separation above a strike-slip fault—are typical of negative flower structures (Harding, 1985; Harding and others, 1985). This is a simple example with poorly developed marginal faults that occurs above a straight, single-stranded fault having an earlier history of strike slip. It is also a very shallow example (less than about 300 m) developed in unconsolidated sediments.

We have considered, and rejected, the possibility that the sag is a velocity push-down produced by overlying slow sediment. It is geologically implausible that such a shallow body of low-velocity sediment would be localized just here where a structural explanation might be reasonable, whereas no such anomaly is present anywhere else along our total of 28 km of reflection profiles in the valley. The surface sediments here are deposits of the Coyote Creek stream system (fig. 14), and thus, if anything, are coarser than elsewhere. Coarser sediment in the Santa Clara Basin section has higher seismic velocity than finer sediment, not lower velocity (Wentworth and Tinsley, 2005b; and see discussion in Shallow Reflection Profiles).

We take this flower structure to indicate continuing strike slip on the Silver Creek Fault in the late Quaternary. Equivalent reflections on either side of the flower structure are at about the same depth, so during this younger period the fault would have experienced strike slip with cross-fault extension, but no dip slip. Quaternary transtension is quite reasonable along the northern Silver Creek Fault, where thrusting

is limited to the eastern side of the basin. Farther south, the cross-fault thrusting may prevent such extension, at least in the shallow crust.

We estimate the age of the sediment at the shallowest imaging of the flower structure (50 m) by projecting stratigraphy downstream and parallel to the Silver Creek Fault from well CCOC to the seismic profile (figs. 2 and 6). This places the 50-m-deep, 138-ka base of alluvial cycle 2 at the shallowest expression of the flower structure, which indicates that the synformal deformation is at least as young as about 140 ka.

Shallow Reflection Profiles

The persistence of the flower structure upward to the shallowest reflections imaged in the minivibroseis profile (fig. 11) suggests that even shallower evidence might be obtainable. The continuity of those reflections shows that subhorizontal layering in the upper 50 m should not be so disrupted as to deny coherent reflections. Efforts to obtain useful shallow data across the Silver Creek Fault have not been particularly successful, however, despite good results in similar materials adjacent to the Coyote Hills to the north (see below).

A shallow seismic reflection profile across the structural sag along the same Jackson Street route in San Jose as the minivibroseis line was collected by R.A. Williams and others in June, 2007. The energy source was a hand-swung, 4.0-kg sledge hammer with "shot" points and receiver spacing of 1 m; the receivers were single 8-Hz vertical seismometers planted in soil or with their geophone spikes wedged tightly into holes in the pavement (table 1).

As seen in figure 12, the reflection results are disappointing. We conclude that the hammer source was not energetic enough for this setting. We see only one clear reflection in the unstacked data (fig. 12*A*). Although a more or less continuous stacked reflection was obtained at each end of the profile (fig. 12*B*), that reflection is irregular and cut by steep abrupt discontinuities. Across the central half of the line no clearly identifiable reflection information was obtained. This absence is difficult to explain, because ambient traffic and radio noise were similar along the whole profile. Possibilities include change in the configuration of buried utilities and, perhaps, poorer source coupling. It is impossible to determine which of the irregularities and disruptions represent reality and which are artificial. As a result, we consider any attempt to use the reflection data from the central part of this profile to be misleading, at best.

On the other hand, the refraction and direct arrival data across the length of this profile are useful for assessing the possibility that lateral change in velocity, rather than structural deformation, has produced the sag as a velocity push down. Like the noisy reflection data described above, the refraction and direct arrivals are also somewhat difficult to interpret, especially in the middle of the sag region.

Despite the noise, we interpret a two-layer case in the upper 10-12 m of the shallow profile: a surficial layer with a P-wave velocity of about 500 m/s that is 3 to about 10 m thick, and an underlying 1,500-m/s layer that probably represents the top of the water table. Both layers appear to be continuous across the length of the profile.

The upper, low-velocity layer clearly thickens, apparently relatively smoothly, from 3-4 m on the edges of the sag to about 10 m in the middle of the sag. This thicker low-velocity zone does cause a local travel time delay, which is also evident in the minivibroseis data. Velocity analysis of the well defined reflection moveout in the minivibroseis data detected the lower velocities, however, and thus permitted compensation for that delay during depth conversion of the data. Persistence of the sag in the resulting depth section (fig. 11) indicates that the synformal sag is real and not a velocity artifact.

Catchings and others (2000) collected a short (600 m) reflection profile across the Silver Creek Fault about 2.25 km to the southeast along the Western Pacific Railroad right-of-way (profile SIT on fig. 2) as a seismic imaging test, using a somewhat more energetic, shotgun source. This profile shows fairly coherent subhorizontal reflections along its length from less than 10 m to a depth of almost 150 m in some places (their fig. 9). The profile indicates detection of reflectors well above 30 m (unusually shallow for a receiver spacing as wide as 5 m) and contains numerous anomalous irregularities, and the report presents no individual shot gathers to illustrate the unstacked reflections. It is thus difficult to assess the validity of the reflections, much less that of the numerous faults that are based on them.

An example of a shallow reflection profile across these alluvial sediments where there are good recording conditions is provided by a short reflection profile (fig. 13) on the outer Niles alluvial fan in a rural area just east of Coyote Hills (GM on figs. 2 and 8). This profile was collected as an equipment test, using a sledgehammer source. Regular, continuous reflections were obtained in the 50-150 millisecond range (approximately 50-150 m deep), with the strong reflection at the bottom representing the top of Franciscan basement. Any systematic reflection terminations or steps in this record could be confidently interpreted as faults, although none are present. Much of the difference between this profile and the Jackson Street hammer profile probably results from the absence of vehicular traffic on or near the profile, better and more consistent source-to-ground coupling of the hammer hitting directly on the soil, and a very high water table.

Possible Stream Capture

Inspection of the distribution of Holocene stream terrace and levee deposits along Coyote Creek (summarized in fig. 14) shows that, at the Evergreen reflection profile, they lie just within the limits of the structural sag over the Silver Creek Fault. If the sag extends along at least the northern part of the fault, then the creek and its deposits might have been captured by an associated topographic sag and held within

18

that depression along much of its lower course. Such capture would constitute evidence that sag deformation producing topographic depression continued into the Holocene. The presence of such a topographic depression in the Holocene seems reinforced by the thickened low-velocity layer within the sag in the upper 10-12 m of section, as described above. This implies accumulation of fine-grained sediment in a depression above the negative flower structure.

Ground-Water Boundary

The sharp subsidence boundary in the InSAR image of figure 15 (Ikehara and others, 1998; Galloway and others, 1999 and 2000) indicates a ground-water barrier along the Silver Creek Fault, and modeling of the ground-water system (Hanson and others, 2004) requires a partial barrier here in the aquifer system below sedimentary cycle 1 (R.T. Hanson, oral commun., 2009). This is consistent with breaks in the reflections approximately beneath the location of the InSAR boundary in the minivibroseis profile, which extend up through the Quaternary section at least to a depth of about 50 m (fig. 11). Whether the barrier extends farther up into or through the uppermost, Holocene layer (cycle 1; above the imaged section in fig. 11) has not been hydrologically tested, and is unknown (R.T. Hanson, oral commun. 2009). It is clear, however, that pumping from cycle 1 in the area is minimal and that the layer is hydrologically separate from the underlying section. This is indicated, for example, by the very limited response of the water level in cycle 1 to pumping in the period December 2000 to December 2001, particularly when compared to the 40-60 ft (12-18 m) seasonal declines measured in the deeper aquifers (Hanson and others, 2002).

Possible Non-Tectonic Causes of Deformation

We should consider the possibility that the shallow expression of the Silver Creek Fault—the dip separation across the base of the Quaternary section and the negative flower structure—might have resulted from entirely nontectonic processes. We consider load compaction in the Evergreen Basin and fault offset or extensional cracking resulting from differential subsidence caused by groundwater withdrawal. We have already considered, and rejected, the possibility that the structural sag results from a velocity pushdown.

It might be possible that the 200 m of dip separation on the base of the Quaternary section across the Silver Creek Fault (fig. 11) resulted from subsidence within the basin as the several-km-thick sedimentary section compacted under its own load. Such compaction in thick sedimentary sections is a well-recognized phenomenon, with the amount dependent on lithology and total thickness. Compaction and associated subsidence has undoubtedly taken place in the Evergreen Basin, but whether 200 m of compaction occurred in the early Quaternary is a separate question. Clearly, none has occurred since.

The base of the Quaternary section is an unconformity, which we recognize within the Evergreen Basin by an abrupt downward increase in seismic velocity. This higher velocity could be due to compaction under an earlier, thick overlying sedimentary section, or possibly to cementation or a different, higher velocity composition. Field observations indicate that the Silver Creek and Packwood Gravels are not extensively cemented, and that, despite being called gravels, they are similar to the Quaternary alluvial section in containing considerable mud and sand as well as gravel. These deposits are distinctly more consolidated than the Quaternary alluvium, however, which is consistent with compaction under an earlier overlying load. This overlying material was removed by erosion in the early Quaternary to form the basal unconformity, and subsequent accumulation of Quaternary alluvium has not reached a thickness sufficient to achieve similar compaction at the base of that overlying section, leaving the velocity step. Because the present load is thus smaller than the pre-unconformity load, we conclude that the underlying sediment in the basin is overconsolidated and not subject to further compaction under the present Quaternary load.

Subsidence caused by withdrawal of ground water might have caused the negative flower structure above the bedrock tip of the Silver Creek Fault, or at least may have enhanced offset across preexisting fault surfaces and possibly caused upward growth of such faults. Ground cracking and fault movement are known to be caused by surface subsidence (Holzer, 1984; Holzer and Galloway, 2005), and the Santa Clara Valley has experienced extensive historical subsidence of the ground surface due to extraction of ground water. This subsidence affected much of the valley, locally reached a total of almost 13 ft (4 m) in San Jose, and for the period 1934-1967 reached maxima greater than 8 ft (2.4 m) in Sunnyvale and San Jose (Poland and Ireland, 1988). The San Jose maximum is bounded on the east by a relatively steep subsidence gradient, which coincides with the even sharper gradient in modern annual subsidence marked by the InSAR boundary and with the location of the underlying Silver Creek Fault (fig. 15).

Attributing the actual formation of the negative flower structure to horizontal extension across the subsidence gradient encounters several problems. The maximum depth of significant groundwater extraction, and therefore of the aquiclude compaction that accomplishes the permanent subsidence, is too shallow to account for the flower structure. Temperature curves for wells CCOC and GUAD show distinct perturbations in the stable geothermal gradient that are caused by groundwater movement (fig. 16), and thus mark the intervals subject to significant groundwater withdrawal. Those in the CCOC temperature log correlate well with the coarse stratigraphic intervals in CCOC, and show that prominent perturbations occur as deep as about 525 ft (160 m), with the deepest perturbation at about 650 ft (198 m). In contrast, however, the negative flower structure extends to almost 1,000 ft (300 m), which is much too deep to have been caused by historical lateral contraction several hundred feet above. The amplitude of the structural sag associated with the flower structure is about 30 m, whereas the maximum observed subsidence elsewhere due to ground-water extraction is 9 m, in the western San Joaquin Valley (Holzer and

Galloway, 2005). If the structural sag developed within the past 100 years as a result of groundwater extraction, there ought to be some evidence of it in the present topography, which there is not. The location of the subsidence gradient, well within the subsidence area, is also a problem. If the flower structure (and the resulting partial groundwater barrier) had not already existed, it seems unlikely that the subsidence gradient would have been localized above the Silver Creek Fault.

Although not the primary cause of rupture, the historical subsidence gradient might have caused movement on or upward propagation of pre-existing tectonic ruptures in the flower structure. We have found no reports of historical surface rupture along the Silver Creek Fault, however, and Poland (1984) reported that he was not aware of any evidence of horizontal movements associated with subsidence in the Santa Clara Valley. A further problem is that the groundwater boundary lies at the west edge of the flower structure, with offsets thus down to the east, whereas any offsets stimulated by the subsidence gradient should be down to the west. We conclude that the subsidence gradient is the result of the flower structure, not its cause, and that it does not seem to have stimulated movement on preexisting fault ruptures. The possibility of such movement might well complicate interpretation of any offsets found by trenching, however, especially any down-to-the-west offsets.

Rate of Fault Offset

We have no basis for estimating the pre-Quaternary rate of strike slip on the Silver Creek Fault, except to suggest that once the Mt. Misery Fault formed, the Silver Creek rate probably decreased or even became sporadic. In the Quaternary, the available constraints are two, the absence of clear evidence of surface faulting and the 200-m dip separation on the base of the Quaternary section. A lack of surface faulting requires a very low rate. In order to use the 200 m of dip separation, which occurred in the early Quaternary phase of fault movement, we assume that the ratio of strike to dip slip involved in the earlier development of the Evergreen Basin can be applied. As previously discussed, this leads to an estimate of less than 2 mm/yr of strike slip during the approximately 1-Ma early Quaternary phase. We have no direct basis for estimating the rate of strike slip responsible for the negative flower structure and so, as a conservative estimate and despite the change to essentially pure strike slip, we assume that the same rate continues in the later Quaternary phase of offset. Any Holocene offset should, at the most, have a similar, very low rate.

Seismicity

The most direct evidence that a fault is active is the occurrence of earthquakes on that fault (although not all active faults exhibit seismicity). The Silver Creek Fault does not show a spatial concentration of earthquakes that would indicate activity, in contrast to the Calaveras Fault, where earthquakes are densely concentrated (fig. 17). The northwest-trending alignment of shallow earthquakes in the southern end of the

Evergreen Basin represent cross-fault shortening (Oppenheimer and others, 1988) largely within several years following the M6.2 Morgan Hill earthquake of 1984, not strike-slip activity on the Silver Creek Fault. The pattern of Calaveras earthquakes does suggest influence from the Silver Creek Fault. At the southeast end of the Silver Creek Fault, the southeast-trending alignment of earthquakes turns abruptly more southward in a 6-degree bend at the Silver Creek junction, and the plan pattern of hypocenters opens up from essentially vertical to very steeply east dipping south of the bend. Either the Silver Creek Fault is still moving, and thus affecting the junction, or the shape of the junction itself is relict from the 2-Ma structural reorganization and has not yet been significantly modified by Calaveras movement.

The lack of abundant small earthquakes along the Silver Creek Fault does not demonstrate that it is inactive, and the location by Bakun (1999 and 2008) of the intensity centers of two M 6.1, 1903 earthquakes near the fault (fig. 17) makes it a possible source. The available constraints for those locations are not sufficient for their confident assignment to the Silver Creek Fault, however, and the earthquakes could have occurred on other fault(s) in the area. Earthquakes of that magnitude should involve about 15 km of fault length each, with offsets of perhaps a half meter each (Wells and Coppersmith, 1994), so that if they had occurred on the 40-km-long Silver Creek Fault, to which we would assign a very low offset rate, then the near-term potential for repetition of such earthquakes on that fault would have been greatly reduced.

Summary and Conclusions

The Silver Creek Fault played a significant, albeit changing role within the San Andreas Fault system for millions of years, and then at about 2 Ma it was abandoned in favor of slip on a northward extension of the Calaveras Fault, as is the case today. Our goal has been to try to determine whether that abandonment was complete or not, and if not, how the fault is now behaving. It is not generating abundant earthquakes, although it is possible that one or both of two M-6.1 earthquakes in 1903 occurred on the fault. In the absence of confident determination from earthquakes, we must turn to the geologic record.

Burial of the northern half of the fault by several hundred meters of Quaternary sediment provides a record of its Quaternary history, and successful imaging of the section by reflection profiling across the fault, together with stratigraphic and paleomagnetic analysis of the section using cores and logs from deep wells, provides a means of reading that record in considerable detail.

Modern gravity data and procedures indicate that a deep basin—the Evergreen Basin—underlies the southeastern Santa Clara Valley and extends for a distance of 40 km northwestward from the Calaveras Fault. The western boundary of this basin is the Silver Creek Fault (not to be confused with the shallow Silver Creek Thrust that overlies the southern part of the basin boundary). Reconstruction of fault offsets by

22

others, using across-fault correlations based both on surface geology and magnetic anomalies, indicates a total of 175 km of right slip in the East Bay fault system, of which about 40 km occurred on the Silver Creek Fault. The Evergreen Basin developed as a pull-apart basin as that 40 km of slip stepped to the right from the Silver Creek Fault to the Hayward Fault. We suggest that an obliquely cross-cutting fault that we call the Mt. Misery Fault then truncated the basin to form a more direct path onto the Hayward Fault, thus accounting for the present southward narrowing of the basin.

We reject past views about the northwestward extent of the Silver Creek Fault and show that it does not extend past the Coyote Hills and beyond as a long strike-slip fault in the San Andreas system. More than 100 km of slip must be accounted for east of the Silver Creek Fault, but the well-positioned Mt. Misery Fault is more than sufficient for that purpose.

The Evergreen reflection profile indicates that Quaternary behavior of the Silver Creek Fault involved two distinct phases. In the early Quaternary, movement continued on the fault sufficient to accomplish 200 m of dip separation on the base of the Quaternary section, which we infer to have accompanied modest strike slip of perhaps less than 2 km, or less than 2 mm/yr. An erosional unconformity that formed about 975 ka truncates this offset and shows only slight dip separation itself, indicating termination of the dip slip motion. A structural sag in the upper Quaternary section that we interpret as a negative flower structure indicates that strike slip continued on the Silver Creek Fault, probably also at a very low rate.

Evidence concerning continuation into the Holocene of this second Quaternary phase of deformation on the Silver Creek Fault is conflicting. The negative flower structure above the fault extends to the upper limit of data in the reflection profile, at a depth of about 50 m and age of about 140 ka, and there is no basis on which to assert that the deformation did not continue. The plan pattern of deposits along Coyote Creek suggests capture of the creek by Holocene topographic depression along the fault over the flower structure, but that is far from definitive. The pattern of earthquakes along the Calaveras Fault suggests continuing influence by the Silver Creek Fault. But there are no confident indicators of fault offset in the Holocene section nor at the ground surface along the fault. We considered the possibility that load compaction within the Evergreen Basin or the historical gradient in surface subsidence across the fault due to withdrawal of ground water were responsible for the offsets in the Quaternary section, but found them lacking. That gradient could, however, complicate interpretation of any evidence of surface offset that might be found.

We suggest, in the absence of good evidence to the contrary, that the Silver Creek Fault probably continues to absorb the kind of right slip that produced the negative flower structure, but at so slow a rate that the shallow faulting, diffused across the width of the flower structure, is not evident at the ground surface, which along the northern part of the fault is within an active depositional system. A very low

rate of slip means that any resultant large earthquakes would also occur very infrequently. If the 1903 earthquakes did, in fact, occur on the Silver Creek Fault, then they would have greatly reduced the short-term future potential for large earthquakes on the fault.

These interpretations of continuing strike slip on the Silver Creek Fault through the Quaternary are founded on the expectation that its predominant style has persisted, inasmuch as its orientation within the San Andreas System remained unchanged. Our estimate of its early Quaternary rate presumes continuation of the ratio of strike- to dip-slip long after the Evergreen Basin was well established, and extrapolation of that same low rate through the late Quaternary, despite the change marked by termination of dip slip, is even less confident and deliberately conservative.

We want to highlight two other issues that emerge from this analysis. The Mt. Misery Fault is a new structural construct, erected both to account for the southward narrowing of the present Evergreen Basin along a straight eastern boundary and to accommodate more than 100 km of the 175 km of right slip that reconstructions of the San Andreas System assign to the East Bay fault system. Little else is known of this fault, except that it is now wholly concealed beneath thrusts at the east side of the Santa Clara Valley. Although we have suggested that it, along with the Silver Creek Fault, was largely abandoned in the 2-Ma structural reorganization, this may not necessarily be the case, and it could well have undergone relatively recent movement. An important corollary is that offset of the western margin of Franciscan terrane across the Calaveras Fault at San Felipe Valley is only about 2-3 km, which since the 2-Ma structural reorganization represents a slip rate of only about one and a half mm/yr, whereas about 15 mm/yr of slip is projected up the Calaveras from the south (California Division of Mines and Geology, 1996; Kelson and others, 2003).

Acknowledgments

References Cited

Andersen, D.W., Metzger, E.P., Ramstetter, N.P., and Shostak, N.C., 2005, Composition of sediment from deep wells in Quaternary alluvium, Santa Clara Valley, California: Geological Society of America, Abstracts with Programs, v. 37, no. 4, p. 37.

Anderson, Megan, Matti, Jonathan, and Jachens, Robert, 2004, Structural model of the San Bernardino basin, California, from analysis of gravity, aeromagnetic, and seismicity data: Journal of Geophysical Research, v. 109, B04404, doi:*10.1029/2003JB002544*.

Bakun, W.H., 1999, Seismic activity of the San Francisco Bay region: Seismological Society of America, Bulletin, v. 898, no. 3, p. 764-784.

Bakun, W.H., 2008, Historical seismicity in the south San Francisco Bay region: U.S. Geological Survey Open-File Report 2008-1151, 37 p., v. 1.1 2008. [*http://pubs.usgs.gov/of/2008/1151/*]

Beyer, L.A., 1980, Borehole gravity program of the U.S. Geological Survey (1963-1975 – brief history and basic data: U.S. Geological Survey Open-File Report 80-903.

Brabb, E.E., and Hanna, W.F., 1981, Maps showing aeromagnetic anomalies, faults, earthquakes epicenters and igneous rocks in the southern San Francisco Bay region: U.S. Geological Survey Geophysical Map GP-932, map scale 1:125,000.

Bryant, W.A., 1981, SE segment of Hayward fault, Evergreen fault, Quimby fault, Silver Creek fault, and Piercy fault: California Division of Mines and Geology Fault Evaluation Report FER-106, 20 p., *in*, Fault evaluation reports prepared under the Alquist-Priolo Earthquake Fault Zoning Act, Region 1 – Central California: California Geological Survey CGS CD 2002-1 (2002), Data CD 2.

Bryant, W.A., and Hart, E.W., 2007, Fault-rupture hazard zones in California: California Geological Survey Special Publication 42, 42 p.

California Department of Water Resources, 1967, Evaluation of ground water resources—South Bay: California Department of Water Resources, Bulletin 118-1, Appendix A, Geology.

California Department of Water Resources, 1968, Evaluation of ground water resources South Bay Fremont study area: California Department of Water Resources, Bulletin 118-1, v. I and v II.

California Department of Water Resources, 1975, Evaluation of ground water resources—south San Francisco Bay: California Department of Water Resources, Bull 118-1, v. III Northern Santa Clara County Area, fig. E, double-page map, scale approximately 1:140,000.

California Division of Mines and Geology, 1982, Earthquake fault zones under the Alquist-Priolo Earthquake Fault Zoning Act, Calaveras Reservoir, Lick Observatory, Morgan Hill, and San Jose East quadrangles: California Geological Survey, Official Earthquake Fault Zone maps, map scale 1:24,000.

California Division of Mines and Geology, 1996, Probabilistic seismic hazard assessment for the State of California: California Division of Mines and Geology Open-File Report 96-08.

Catchings, R.D., Borchers, J.W., Goldman, M.R., Gandhok, G., Ponce, D.A., and Steedman, C.E., 2006, Subsurface structure of the East Bay plain ground-water basin—San Francisco Bay to the Hayward Fault, Alameda County, California: U.S. Geological Survey Open-File Report 2006-1084 [*http://pubs.usgs.gov/of/2006/1084/*].

Catchings, R.D., Goldman, M.R., Gandhok, G., Rymer, M.J., and Underwood, D.H., 2000, Seismic imaging evidence for faulting across the northwestern projection of the Silver Creek fault, San Jose, California: U.S. Geological Survey Open-File Report 2000-125.

Catchings, R.D., Rymer, M.J., and Goldman, M.R., 2009, The Silver Creek Fault in Downtown San Jose, Santa Clara County, California: Seismological Research Letters v. 80, no. 2, p. 375.

Crittenden, M.D., Jr., 1951, Geology of the San Jose-Mount Hamilton area: California: California Division of Mines, Bulletin 157, map scale 1:62,500, 74 p.

Galloway, Devin, Jones, D.R., and Ingebritsen, S.E., eds., 1999, Land subsidence in the United States: U.S. Geological Survey Circular 1182.

Galloway, D.L., Jones, D.R., and Ingebritsen, S.E., 2000, Measuring land subsidence from space: U.S. Geological Survey, Fact Sheet-051-00 [*http://pubs.usgs.gov/fs/fs-051-00/*].

Graymer, R.W., 2000, Geologic map and map database of the Oakland metropolitan area, Alameda, Contra Costa, and San Francisco Counties, California: U.S. Geological Survey Miscellaneous Field Studies Report MF-2342, map scale 1:50,000.

Graymer, R.W., McLaughlin, R.J., Stanley, R.G., Ponce, D.A., Jachens, R.C., Simpson, R.W., and Wentworth, C.M., 2005, Santa Clara Valley-bounding faults characterized by structural superposition: Geological Society of America, Abstracts with Programs, v. 37, no. 4, p. 58.

Graymer, R.W., Sarna-Wojcicki, A.M., Walker, J.P., McLaughlin, R.J., and Fleck, R.J., 2002, Controls on timing and amount of right-lateral offset on the East Bay fault system, San Francisco Bay region, California: Geological Society of America Bulletin, v. 114, p. 1471-1479.

Hanson, R.T., Newhouse, M.W., Wentworth, C.M., Williams, C.F., Noce, T.E., and Bennett, M.J., 2002, Santa Clara Valley Water District multi-aquifer monitoring-well site, Coyote Creek Outdoor Classroom, San Jose, California: U.S. Geological Survey Open-File Report 02-369.

Hanson, R.T., Zhen, Li, and Faunt, C.C., 2004, Documentation of the Santa Clara Valley regional ground-water/surface-water flow model, Santa Clara County, California: U.S. Geological Survey Scientific Investigations Report 2004-5231, 75 p.

Harding, T.P., 1985, Seismic characteristics and identification of negative flower structures, positive flower structures, and positive structural inversion: Association of Petroleum Geologists Bulletin, v. 69, p. 582-600.

Harding, T.P., Vierbuchen, R.C., and Christie-Blick, Nicholas, 1985, Structural styles, plate-tectonic settings, and hydrocarbon traps of divergent (transtensional) wrench faults, *in*, Biddle, K.T., and Christie-Blick, Nicholas, eds., Strike-slip deformation, basin formation, and sedimentation: Society of Economic Paleontologists and Mineralogists, Special Publication No. 37, p. 51-77.

Hazelwood, R.M., 1974, Preliminary report of seismic refraction survey along the east side of the San Francisco Bay, Alameda County, California: U.S. Geological Survey Open-File Report [no OFR number].

Hazelwood, R.M., 1976, Contour map and interpretive cross sections showing depth and configuration of bedrock surface, South San Francisco Bay region, California: U.S. Geological Survey Miscellaneous Fields Studies Map MF-796, map scale 1:62,500.

Hitchcock, C.S., and Brankman, C.M., 2002, Assessment of late Quaternary deformation, eastern Santa Clara Valley, San Francisco Bay region: U.S. Geological Survey, National Earthquake Hazards Reduction Program, Final Technical Report, Award Number 01HQGR0034, 46 p.

Holzer, T. L., 1984, Ground failure induced by groundwater withdrawal from unconsolidated sediments, *in*, Holzer, T.L., ed., Reviews in Engineering Geology: Geological Society of America v. VI, p. 67-105.

Holzer, T.L., and Galloway, D.L., 2005, Impacts of land subsidence caused by withdrawal of underground fluids in the United States, *in* Ehlen, J., Haneberg, W.C., and Larson, R.A., eds., Humans as geologic agents: Geological Society of America Reviews in Engineering Geology, v. 16, p. 87-99, doi:*10.1130/2005.4016(08)*.

Ikehara, M.E., Galloway, D.L., Burgmann, Roland, and Lewis, A.S., 1998, InSAR imagery reveals seasonal and longer-term land-surface elevation changes influenced by ground-water levels and fault alignment in Santa Clara Valley, California: Eos, Transactions, American Geophysical Union, v. 79, p. 937.

Jachens, R.C., Wentworth, C.M., Graymer, R.W., McLaughlin, R.J., and Chuang, F.C., 2002, A 40-km-long concealed basin suggests large offset on the Silver Creek fault, Santa Clara Valley, California, Geological Society of America Abstracts with Programs, v. 34, no. 5, p. A99.

Jachens, R.C., and Moring, B.C., 1990, Maps of thickness of Cenozoic deposits and the isostatic residual gravity over basement for Nevada: U.S. Geological Survey Open-File Report 90-404, 2 sheets, map scale 1:1,000,000.

Jachens, R.C., Wentworth, C.M., Graymer, R.W., Stanley, R.G., McLaughlin, R.J., Simpson, R.W., Williams, R.A., Andersen, D.W., Ponce, D.A., and Langenheim, V.E., 2005, Late Cenozoic stratigraphic and tectonic history of the Santa Clara Valley, California [abs.]: Geological Society of America, Abstracts with Programs, v. 37, no. 4, p. 59.

Jennings, C.W., and Burnett, J.L., 1961, Geologic map of California , San Francisco Sheet: California Division of Mines, Geologic Map of California, map scale 1:250,000.

Jennings, C.W., and Saucedo, G.J., 1994, Fault activity map of California and adjacent areas: California Division of Mines and Geology, California Geologic Data Map Series, Map no. 6, map scale 1:750,000.

Kelson, K.I., Baldwin, J.N., and Brankman, C.M., 2003, Late Holocene displacement of the central Calaveras Fault, Furtado Ranch site, Gilroy, CA: U.S. Geological Survey, National Earthquake Hazards Reduction Program, Award Number 01-HQ-GR-0124, Final Technical Report.

Leighton, A., Fio, J.L., and Metzger, L.F., 1995, Database of well and areal data, south San Francisco Bay and Peninsula area, California: U.S. Geological Survey Water-Resources Investigations Report 94-4151.

McLaughlin, R.J., Sliter, W.V., Sorg, D.H., Russell, P.C., and Sarna-Wojcicki, A.M., 1996, Large-scale right-slip displacement on the East San Francisco Bay Region fault system, California—Implications for location of late Miocene to Pliocene Pacific plate boundary: Tectonics, v. 15, p. 1-18.

Mankinen, E.A., and Wentworth, C.M., 2003, Preliminary paleomagnetic results from the Coyote Creek Outdoor Classroom drill hole, Santa Clara Valley, California: U.S. Geological Survey Open-File Report 03-187, 32 p. [*http://pubs.usgs.gov/of/2003/of03-187/*].

Marlow, M.S., Jachens, R.C., Hart, P.E., Carlson, P.R., Anima, R.J., and Childs, J.R., 1999, Development of San Leandro synform and neotectonics of the San Francisco Bay block, California: Marine and Petroleum Geology, v. 16, p. 431-442.

Mascarelli, A.L., 2009, Quaternary geologists win timescale vote: Nature, v. 459, 4 June 2009, p. 624.

Mathews, V., III, 1976, Correlation of the Pinnacles and Neenach volcanic formations and their bearing on San Andreas fault problems: American Association of Petroleum Geologists Bulletin, v. 60, p. 2128-2141.

Michael, A. J., 1988, Effects of three-dimensional velocity structure on the seismicity of the 1984 Morgan Hill, CA aftershock sequence, Bulletin Seismological Society of America, v. 78, p. 1199-1221.

Nakata, J.K., Sorg, D.H., Russell, P.C., Meyer, C.E., Wooden, J., Lanphere, M.A., McLaughlin, R.J, Sarna-Wojcicki, A.M., Saburomaru, J.Y., Pringle, M.S., and Drinkwater, J., 1993, New radiometric ages and tephra correlations from the San Jose and the northeastern part of the Monterey 1:100,000 map quadrangles, California: Isochron/West, v. 60, P. 19-32.

Newhouse, M.W., Hanson, R.T., Wentworth, C.M., Everett, R.R., Williams, C.F., Tinsley, J.C., Noce, T.E., and Carkin, B.A., 2004, Geologic, water-chemistry, and hydrologic data from multiple-well monitoring sites and selected water-supply wells in the Santa Clara Valley, California, 1999-2003: U.S. Geological Survey, Scientific Investigations Report 2004-5250 [*http://pubs.usgs.gov/sir/2004/5250/*].

Oppenheimer, David H., Reasenberg, Paul A., and Simpson, Robert W., 1988, Fault Plane Solutions for the 1984 Morgan Hill, California, Earthquake Sequence: Evidence for the State of Stress on the Calaveras Fault: Journal of Geophysical Research, v. 93, no. B8, p. 9007–9026.

Pampeyan, E.H., 1979, Preliminary map showing recency of faulting in coastal north-central California: U.S. Geological Survey Miscellaneous Field Studies Map MF-1070, map scale 1:250,000.

Poland, J.F., 1971, Land subsidence in the Santa Clara Valley, Alameda, San Mateo, and Santa Clara Counties, California: U.S. Geological Survey Open-File Report, map scale 1:125,000 (San Francisco Bay Region Environment and Resources Planning Study, Technical Report 2).

Poland, J.F., 1984, Case history No. 9.14. Santa Clara Valley, California, U.S.A., *in*, Poland, J.F., ed., Guidebook to studies of land subsidence due to ground-water withdrawal: United Nations Educational, Scientific and Cultural Organization (Unesco), International Hydrological Programme, Working Group 8.4, p. 279-290.

Poland, J.F., and Ireland, R.L., 1988, Land subsidence in the Santa Clara Valley, California, as of 1982: U.S. Geological Survey Professional Paper 497-F, 61 p.

Roberts, C.W., and Jachens, R.C., 2003, Shaded relief aeromagnetic map of the Santa Clara Valley and vicinity, California: U.S. Geological Survey Open-File Report 03-360, map scale 1:100,000.

Rogers, T.H., 1966, Geologic map of California, San Jose sheet: California Division of Mines and Geology, map scale 1:250,000.

Ross, D.C., 1970, Quartz gabbro and anorthositic gabbro: markers of offset along the San Andreas fault in the California Coast Ranges: Geological Society of America Bulletin, v. 81, p. 3647-3662.

Simpson, R.W., Graymer, R.W., Jachens, R.C., Ponce, D.A., and Wentworth, C.M., 2004, Cross-sections and maps showing double-difference relocated earthquakes from 1984-2000 along the Hayward and Calaveras Faults, California: U.S. Geological Survey, Open-File Report 2004-1083 [*http://pubs.usgs.gov/of/2004/1083/*].

Snetsinger, K.G., 1976, Rock types of the Franciscan Formation, Coyote Hills, Alameda County, California: California Geology, August, 1976, p. 174-177.

Stanley, R.G., Jachens, R.C., Lillis, P.G., McLaughlin, R.J., Kvenvoldeen, K.A., Hostettler, F.D., McDougall, K.A., and Magoon, L.B., 2002, Subsurface and petroleum geology of the southwestern Santa Clara Valley ("Silicon Valley"), California: U.S. Geological Survey Professional Paper 1663.

Stanley, R.G., Wentworth, C.M., Williams, R.A., Jachens, R.C., Graymer, R.W., Catchings, R.D., McLaughlin, R.J., Lillis, R.G, White, L.D., and Valin, Z.C., 2005, Concealed sedimentary basins beneath the Santa Clara Valley, California [abs.]: Geological Society of America, Abstracts with Programs, vol.37, no. 4, pp. 57.

Taylor, S.G. Jr., 1956, Gravity investigation of the southern San Francisco Bay area, California: Stanford University unpub. Ph.D. thesis, 105 p.

Wagner, D.L, Bortugno, E.J., and McJunkin, R.D., 1991, Map showing recency of faulting, San Francisco-San Jose Quadrangle, 1:250,000: California Division of Mines and Geology, Regional Geologic Map Series, Map No. 5A (Geology), Sheet 5, map scale 1:250,000.

Waldhauser, Felix, and Schaff, D.P., 2008, Large-scale relocation of two decades of Northern California seismicity using cross-correlation and double-difference methods: Journal of Geophysical Research, v. 113, B08311, doi:*10.1029/2007JB005479*.

Walker, J.D., and Geissman, J.W., compilers, 2009, Geologic time scale: Geologic Society of America, doi:*1130/2009.CTS004R2C*.

Wells, D.L., and Coppersmith, K.J., 1994, New empirical relationships among magnitude, rupture length, rupture width, and surface displacements: Bulletin of the Seismological Society of America, v. 84, p. 974-1002.

Wentworth, C.M., Blake, M.C., Jr., McLaughlin, R.J., and Graymer, R.W., 1998, Preliminary geologic map of the San Jose 30 X 60-minute quadrangle, California—a digital database: U.S. Geological Survey Open-File Report 98-795, map scale 1:100,000.

Wentworth, C.M., and Tinsley, J.C., 2005a, Tectonic subsidence and cyclic Quaternary deposition controlled by climate variation, Santa Clara Valley, California [abs.]: Geological Society of America, 2005 Abstracts with Program.

Wentworth, C.M., and Tinsley, J.C., 2005b, Geologic setting, stratigraphy, and detailed velocity structure of the Coyote Creek borehole, Santa Clara Valley, California, in, Asten, M.W., and Boore, D.M., eds., Blind comparisons of shear-wave velocities at closely spaced sites in San Jose, California: U.S. Geological Survey Open-File Report 2005-1169, part 2_01, 26 p. [*http://pubs.usgs.gov/of/2005/1169/*].

Wentworth, C.M., Tinsley, J.C., Andersen, D.W., Graham, S.E., Jachens, R.C., Mankinen, E.A., and Williams, R.A., 2005, Quaternary deposits of the Santa Clara Valley, California [abs.]: Geological Society of America, Abstracts with Programs, v. 37, no. 4, pp. 58.

Williams, C.F., Galanis, S.P., Jr., Brubb, F.V., and Moses, T.H., Jr. 1994, The thermal regime of Santa Maria Province, California: U.S. Geological Survey Bulletin 1995-F (available only as Bulletin 1995-F-G).

Williams, R.A., Stephenson, W.J., Wentworth, C.M., Odum, J.K., Hanson, R.T., Jachens, R.C., 2002, Definition of the Silver Creek Fault and Evergreen Basin Sediments From Seismic Reflection Data, San Jose, California [abs.]: Eos Trans. AGU, 83(47), Fall Meet. Suppl., Abstract T71E-1207, 2002.

Witter, R.C., Kelson, K.I., Barron, A.D., and Sundermann, S.T., 2003, Map of active fault traces, geomorphic features and Quaternary surficial deposits along the central Calaveras fault, Santa Clara County, California: U.S. Geological Survey, National Earthquake Hazards Reduction Program Final Technical Report, [Grant award number 01HQGR0212], 32 p.

Witter, R.C., Knudsen, K.L, Sowers, J.M., Wentworth, C.M., Koehler, R.D., Randolph, C. E., Brooks, S.K., and Gans, K.D., 2006, Maps of Quaternary deposits and liquefaction susceptibility in the central San Francisco Bay region, California: U.S. Geological Survey Open-File Report 06-1037 [*http://pubs.usgs.gov/of/2006/1037/*].

Table 1 - Data acquisition parameters for Jackson St. Minivibroseis and hammer reflection profiles.

Parameter	Jackson St. Minivibroseis	Jackson St. Hammer
Seismic source:	9990-kg MiniVibe II	4-kg sledgehammer
Sweep parameters:	10-200 Hz; 4-8 sweeps, 14-s sweeps	single impact; stack 4
Source point interval:	10.0 m	1.0 m
Geophones:	Single, 8-Hz vertical geophone	Single, 8-Hz vertical geophones
Geophone interval:	5.0 m	1.0 m
Recording geometry:	240-channel linear array	96-192 channel linear array
Near trace offset:	5.0 m	0.0 m
Recording filters:	None	none
Recording system:	Geometrics Geode	Geometrics Geode
Sampling interval:	0.001 s	0.0005 s
Record length:	2.0 s	1.0 s
Recording format:	SEG-2	SEG-2

Minivibroseis Data Processing Sequence:

Data reformat: convert from SEG-2 to ProMAX® internal
AGC - 200 ms window
Trace edit: delete noisy traces
Zero all data amplitudes in the surface-wave arrival zone
Velocity attenuator on 490 m/s coherent noise
Common midpoint (CMP) sort: nominally 60 fold
Elevation statics - 1200 m/s correction velocity
Normal moveout correction (NMO), 70% stretch mute
Band-pass filter: 15-30-80-120 Hz and 60-Hz notch
Residual statics - 10 ms maximum shift
CMP stack
Predictive Deconvolution filter: 180 ms operator length
Frequency-distance (F/X) deconvolution filter 10-100 Hz pass band; 11 trace window
Kirchoff finite-difference time migration
Time-to-depth conversion: smoothed velocity function

Hammer Data Processing Sequence:

Data reformat: convert from SEG-2 to ProMAX internal
Surface Wave noise attenuation: targeting coherent noise at 550 m/s
AGC 200 ms window
Band-pass filter: 50-100-200-300 Hz and 135-Hz notch
Elevation statics - 400 m/s correction velocity
Zero all data amplitudes in the surface-wave arrival zone
Frequency-wavenumber (FK) filter targeting radio noise with velocities above -4000 to 4000 m/s
Common midpoint (CMP) sort: nominally about 60 fold
Velocity analysis - Normal moveout correction (NMO), 30% stretch mute
Top mute
FK filter targeting coherent noise in the range of -700 to 700 m/s
CMP stack
Trace Mix – 9 traces
Band-pass filter: 50-100-200-300 Hz
FK fan filter attenuating velocities from -700 to 700 m/s
F/X deconvolution filter: 10-200 Hz, 11-trace horizontal window
Time-to-depth conversion
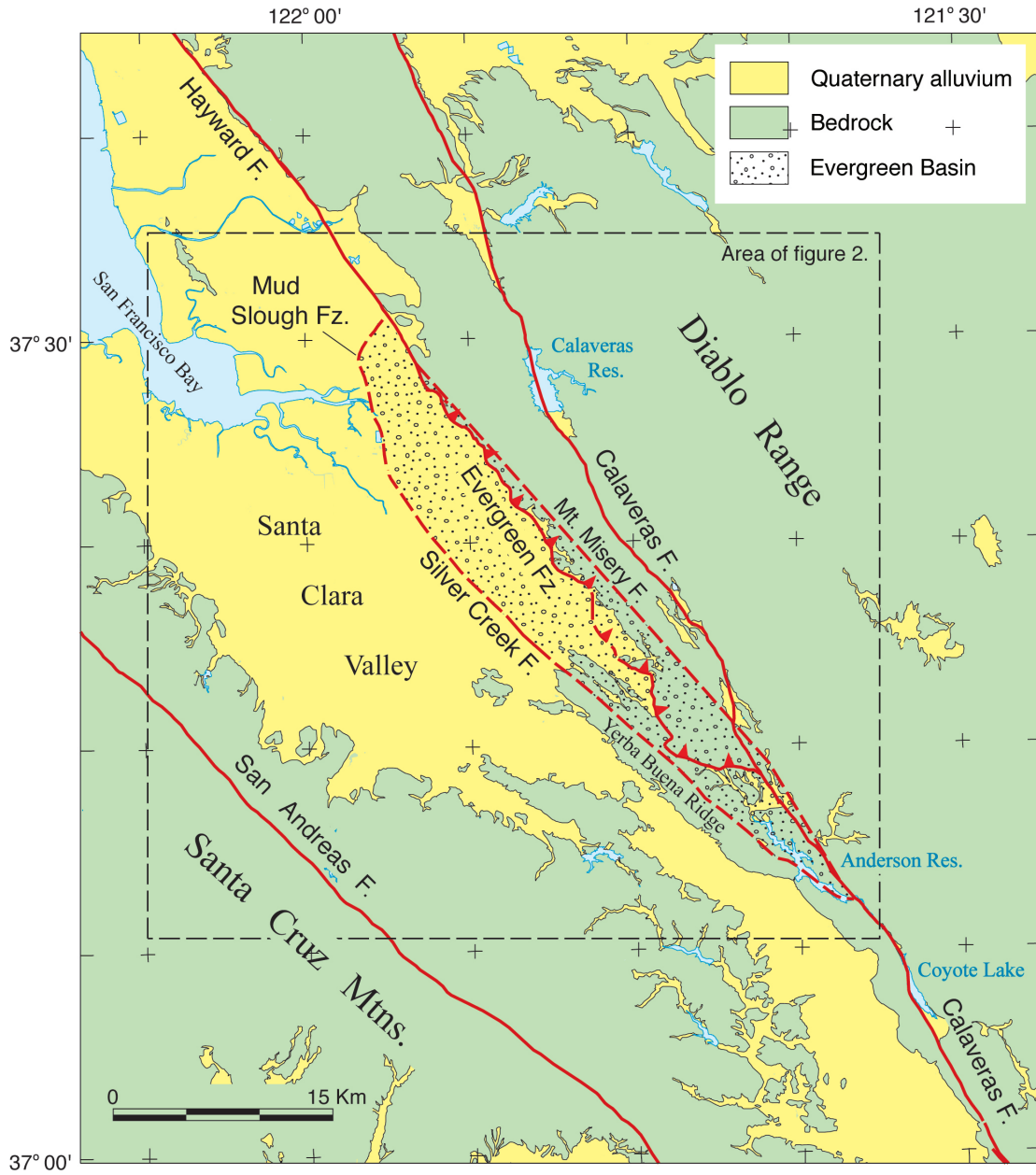
Figure 1. Index map of the Santa Clara Valley, California, area showing selected faults (F.) and fault zones (Fz.), and the Evergreen Basin. Faults are dashed where concealed. Faults on the southwest side of Santa Clara Valley are not shown.
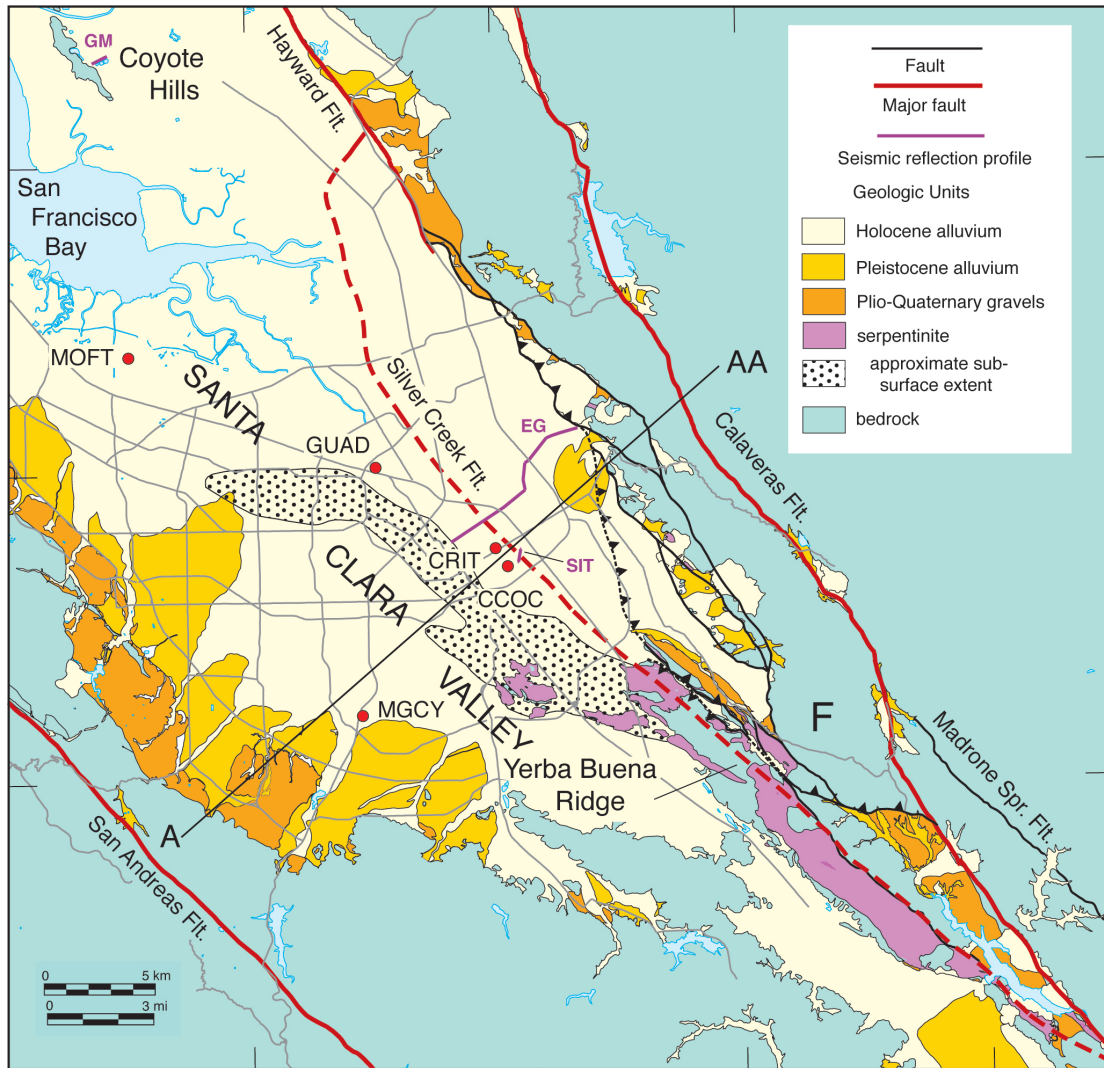
Figure 2. Geologic setting of the Silver Creek Fault, Santa Clara Valley, California, showing principal faults of the San Andreas system, the locations of drill holes MOFT (Moffett), GUAD (Guadalupe), CCOC (Coyote Creek), MGCY (McGlincy), water well CRIT (Crittenden), and seismic reflection lines Evergreen (EG; Williams and others, 2002), seismic imaging test (SIT; Catchings and Others, 2000), and Geometrics (GM; fig. 13). See figure 3 for cross section A-AA. F marks the overthrust flap of Mesozoic rocks. Dashed and dotted faults are concealed. Teeth shown on selected thrusts to emphasize structure. Faults on the southwest side of Santa Clara Valley are not shown. Approximate subsurface extent of major serpentinite sheet based on aeromagnetic anomaly (Roberts and Jachens, 2003). Main roads shown in the Santa Clara Valley.
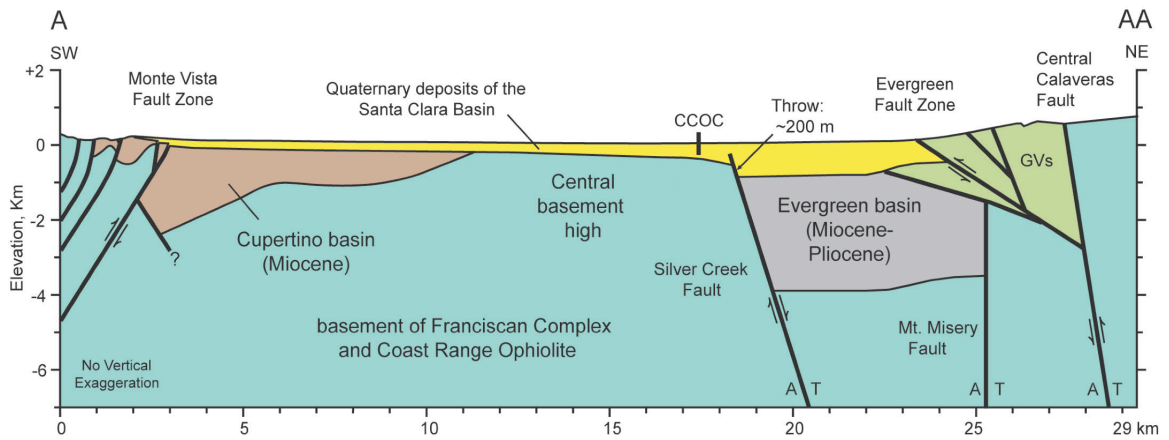
Figure 3. Schematic cross section A-AA across the Santa Clara Valley, California (see fig. 2 for location). Note the Evergreen Basin and schematic version of its bounding faults, including shallow thrusts. GVs; Great Valley sequence. Based on a figure used by Stanley and others (2005).
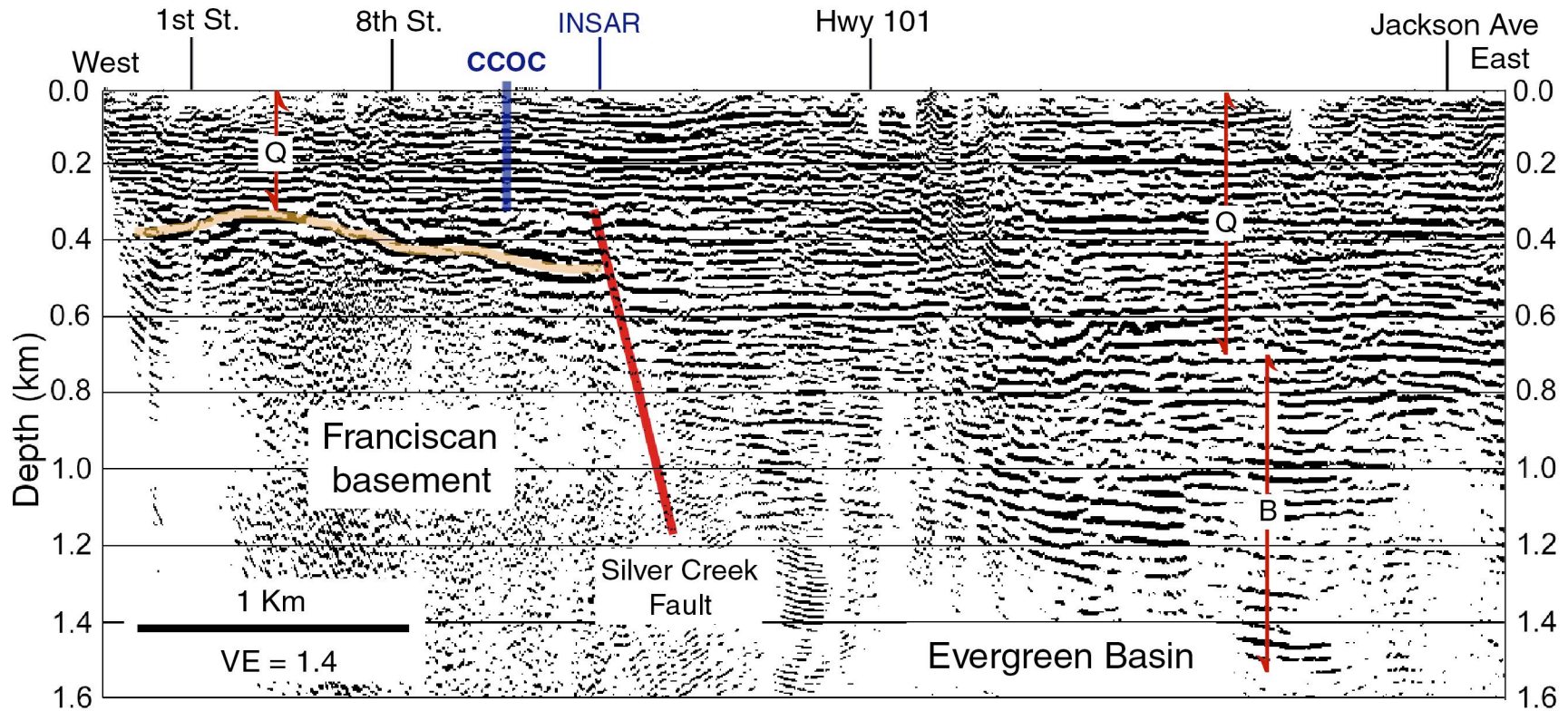
Figure 4. Evergreen minivibroseis seismic reflection profile (migrated) along Jackson Street and eastward in San Jose, California (see figs. 2 and 8 for location), showing basement reflection (orange) and steeply east-dipping Silver Creek Fault. Note the subhorizontal layering across most of the profile, the strong reflection at the top of Franciscan basement, its abrupt termination at the Silver Creek Fault, the layered reflections that extend well below that basement surface within the Evergreen Basin, and their westward termination at the Silver Creek Fault. Q, Quaternary alluvial sediment, B, sedimentary fill of the Evergreen Basin. Vertical scale is depth in km. See figure 11 for details around the Silver Creek Fault. The easternmost 2.5 km of the original profile are not shown here.
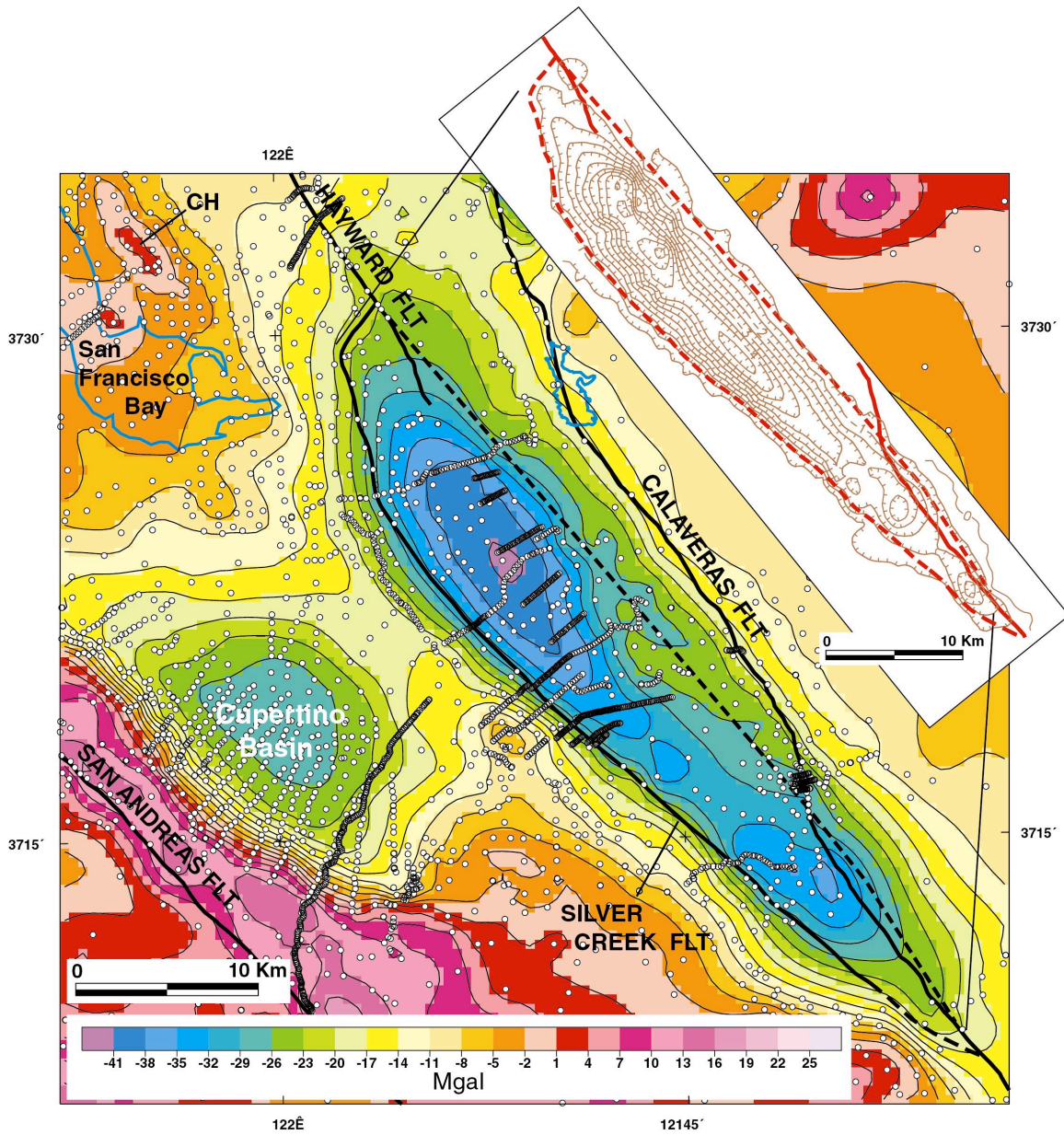
Figure 5. Map of isostatic residual gravity and selected faults showing prominent gravity lows marking the Cupertino Basin (left) and the northwest-trending Evergreen Basin (center), California. The Coyote Hills produce the small, elongate high at upper left (CH). Contour interval 3 milligals. Small circles mark gravity stations. Inset shows basin thickness inversion (as elevation) for the Evergreen Basin; contour interval 0.5 km, and the basin-bounding faults.
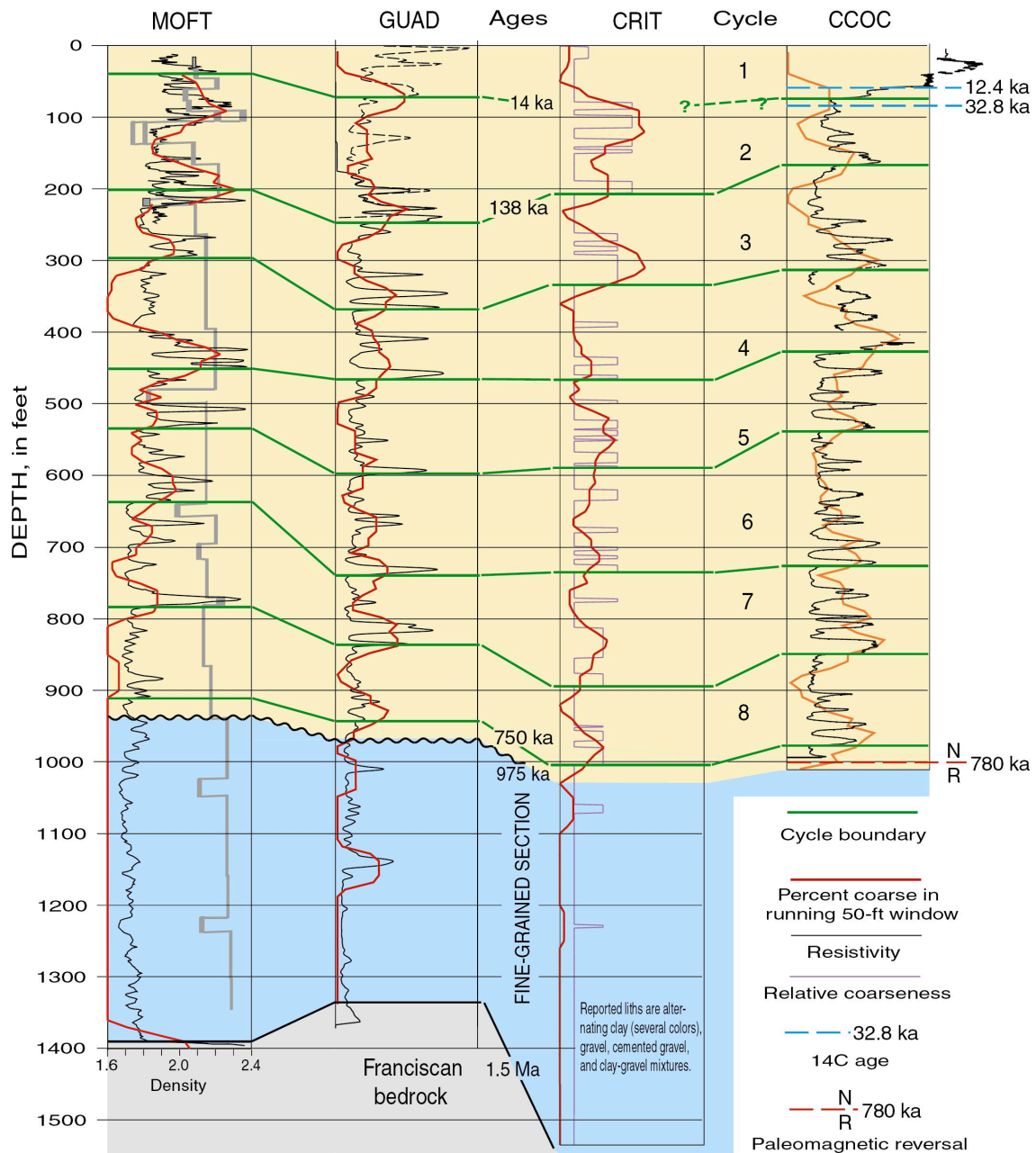
Figure 6. Quaternary alluvial section beneath the central Santa Clara Valley, California, as represented in four wells: Moffett (MOFT), Guadalupe (GUAD), Coyote Creek (CCOC), and a deep water well (CRIT) described by Crittenden (1951) (see fig. 2 for locations). Franciscan basement was reached at a depth of 1,390 ft (424 m) in MOFT and 1,336 ft (407 m) in GUAD; CRIT bottomed at 1,535 ft (468 m) in clay. Details of the section for MOFT, CCOC, and GUAD are represented by resistivity logs (black), and for CRIT by a curve of relative coarseness (purple) representing each driller-described interval. A density curve (gray) based on a downhole gravimeter survey (Beyer, 1980) is also shown for MOFT. The red curves show average coarseness of the section in a running 50-ft-high window (15 m).
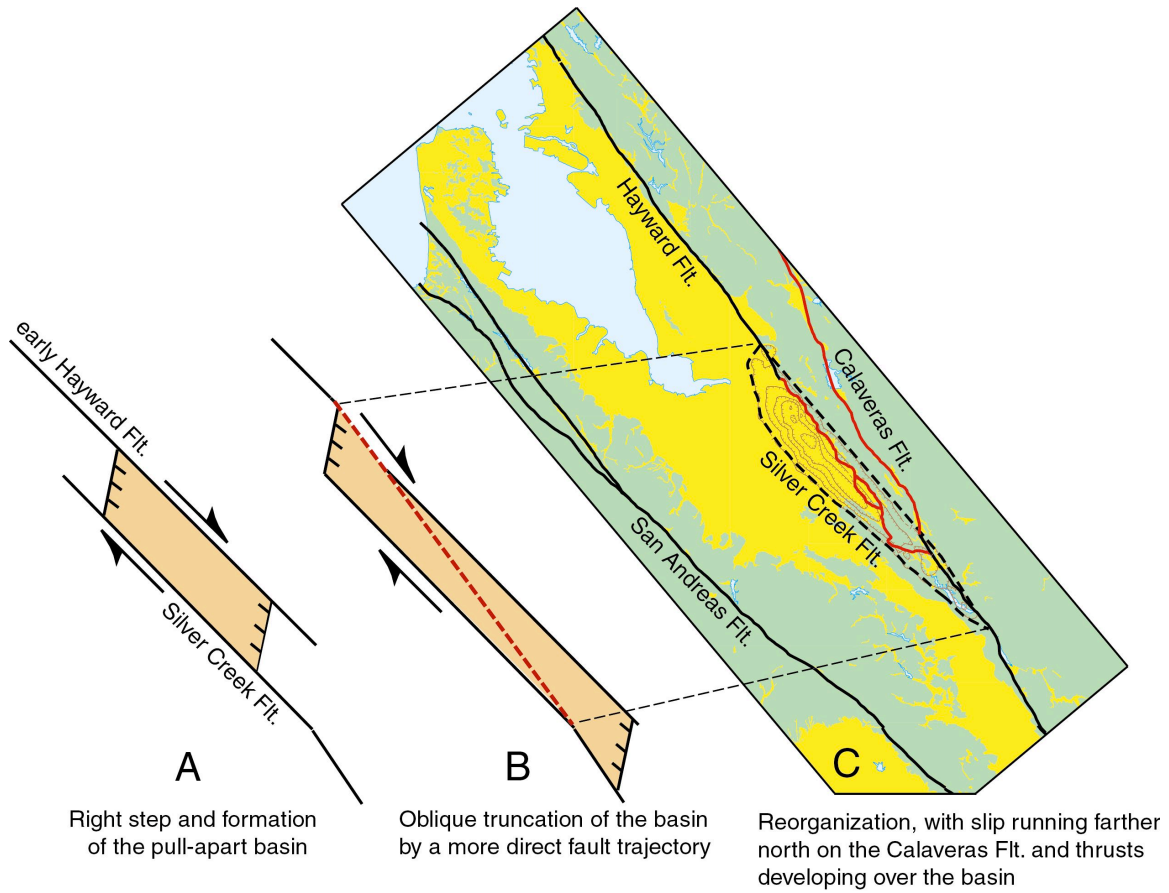
Figure 7. Maps showing the structural progression from (*A*) initial formation of the Evergreen pull-apart basin across a right step between the Silver Creek and Hayward Faults, through (*B*) the oblique truncation of that basin by a new fault (Mt. Misery Fault), to (*C*) the abandonment of the Silver Creek and Mt. Misery Faults in favor of a northward extension of the central Calaveras Fault and development of thrusting over the Evergreen Basin. New faults in stages *B* and *C* shown in red.
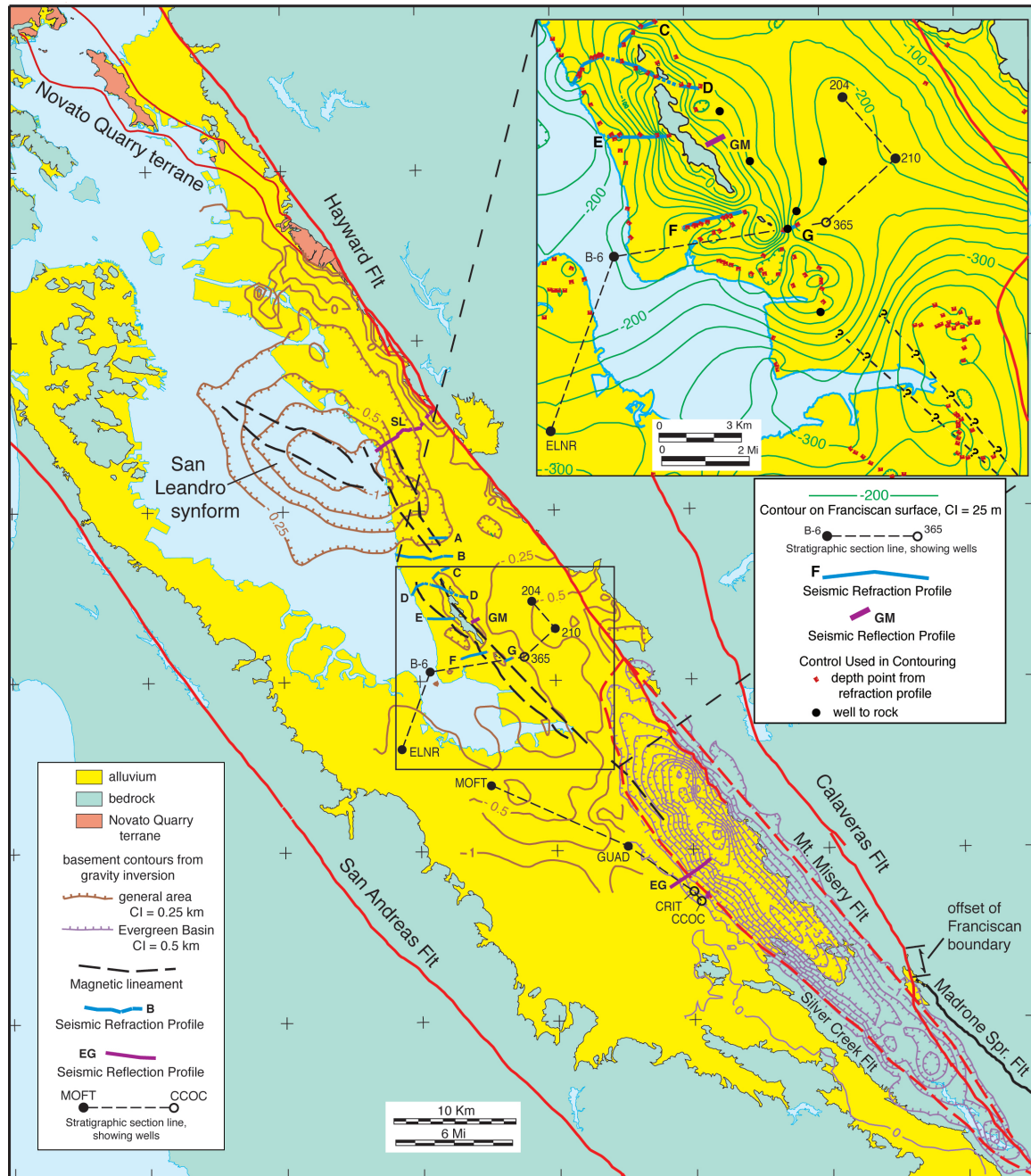
Figure 8. Map showing constraints on any possible northwestward extension of the Silver Creek Fault, California. Range of possible northwest trajectories of the fault shown in the inset by queried dashed lines. Elevation contours on the basement surface from basin inversion of gravity and (inset) by gridding and contouring of well and refraction control. Paired magnetic lineaments mark the boundaries of elongate magnetic rock bodies. Refraction profiles (labeled A to G) from Hazelwood, 1974 and 1976 (see fig. 10). Reflection profiles: EG; Evergreen (see fig. 4); GM; Geometrics (see fig. 13); SL; San Leandro profile of Catchings and others, 2006. See figure 6 for stratigraphic section MOFT-CCOC, and figure 9 for ELNR-204. Novato Quarry terrane from Graymer, 2000.
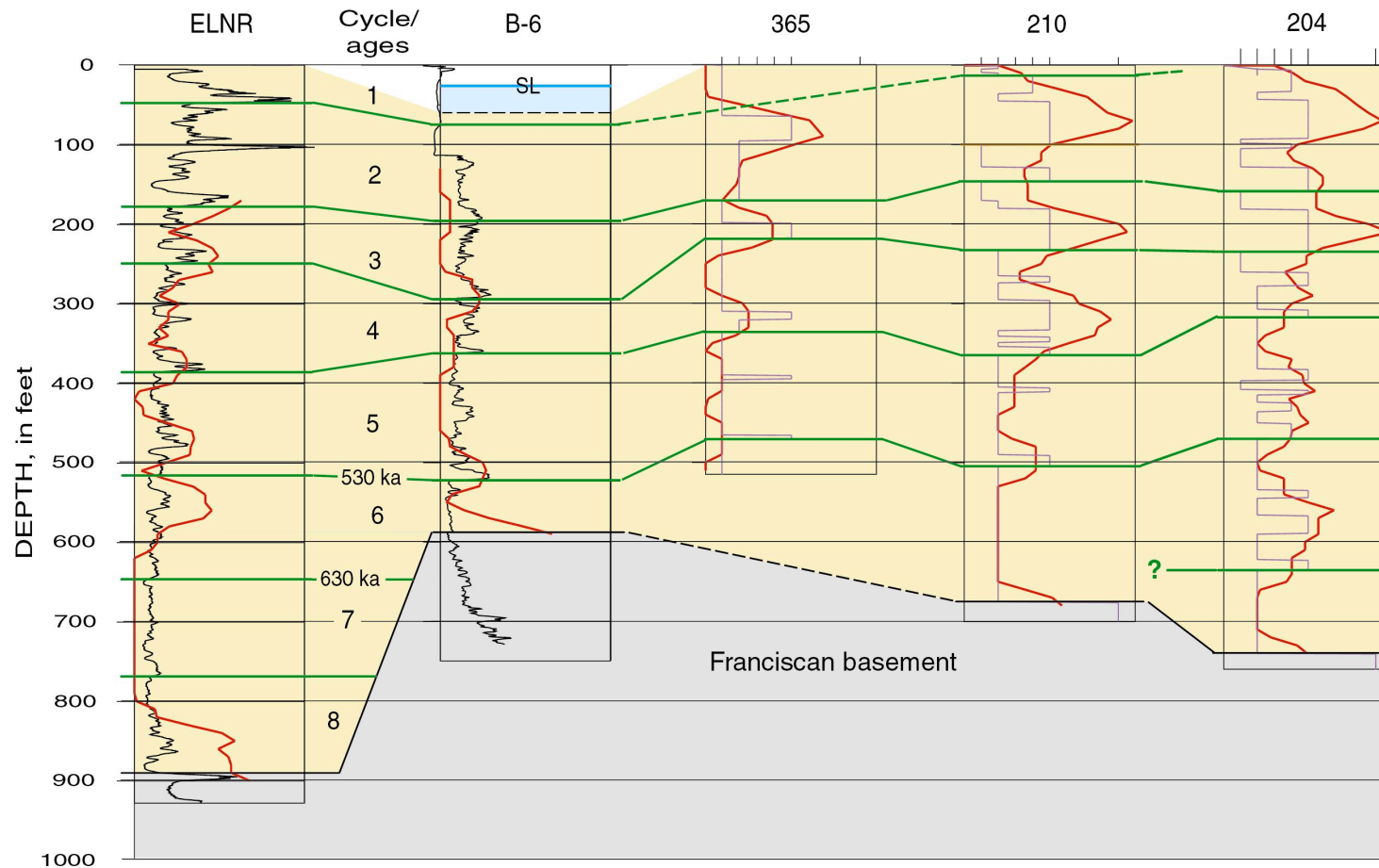
Figure 9. Stratigraphic section across the southern San Francisco Bay and Coyote Hills, California, showing the alluvial sequence that inundates the early Quaternary erosion surface. The crest of the Coyote Hills lies between wells B-6 and 365. See figure 8 for section line and wells. Compare with figure 6 to see correlation southward into the central Santa Clara Basin. Well B-6 was drilled from a bridge over the Bay such that sea level (SL) and the Bay bottom are included within the well log.
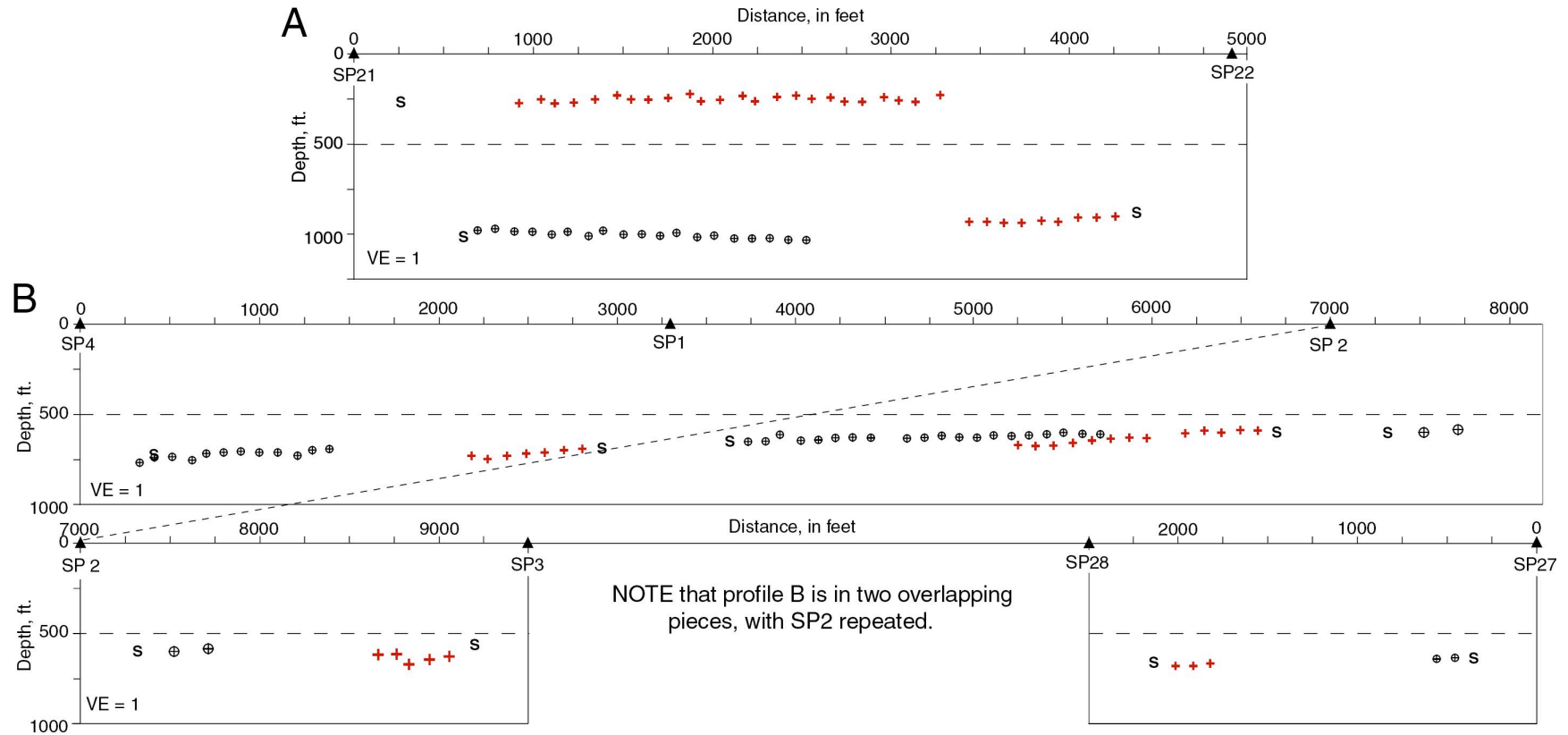
Figure 10. (page 1 of 3) Depth and shape of the basement surface near Coyote Hills, California, determined by seismic refraction profiling (Hazelwood, 1974 and 1976). Profile locations shown on figure 8. Reversed profiles were collected using small explosive charges placed about 25 ft (7.6 m) deep in boreholes and with a geophone spacing of 100 ft (30.5 m). Most profiles represent a two-layer problem in which the velocity of the upper, sediment layer is 5,500 ft/s (1,675 m/s) and that of the lower, basement layer averages about 12,000 ft/s (3.7 km/s, appropriate for shallow Franciscan rock). [caption continued on next page]
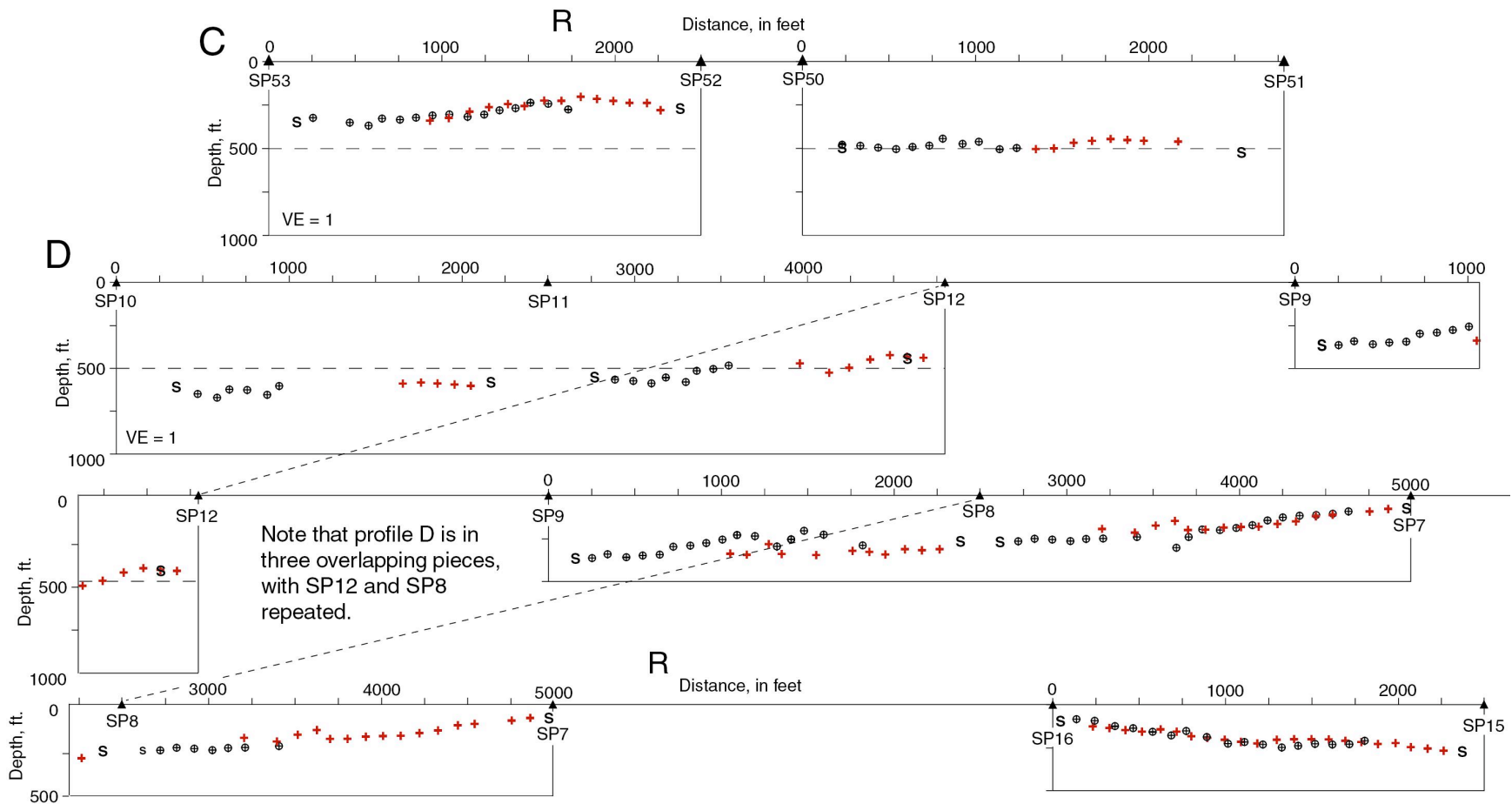
Figure 10. (page 2 of 3). [continued] Migrated depth points along the top of the lower refractor were calculated as wave entrance points (shown by S symbols) and then as exit points up to each geophone (shown by red symbols where to the right of the shot point and black symbols where to the left). A consistent solution requires that the S symbols lie along the same surface as the other depth points. Profile A represented a more complex, three-layer problem, which Hazelwood treated in two steps. [caption continued on next page]
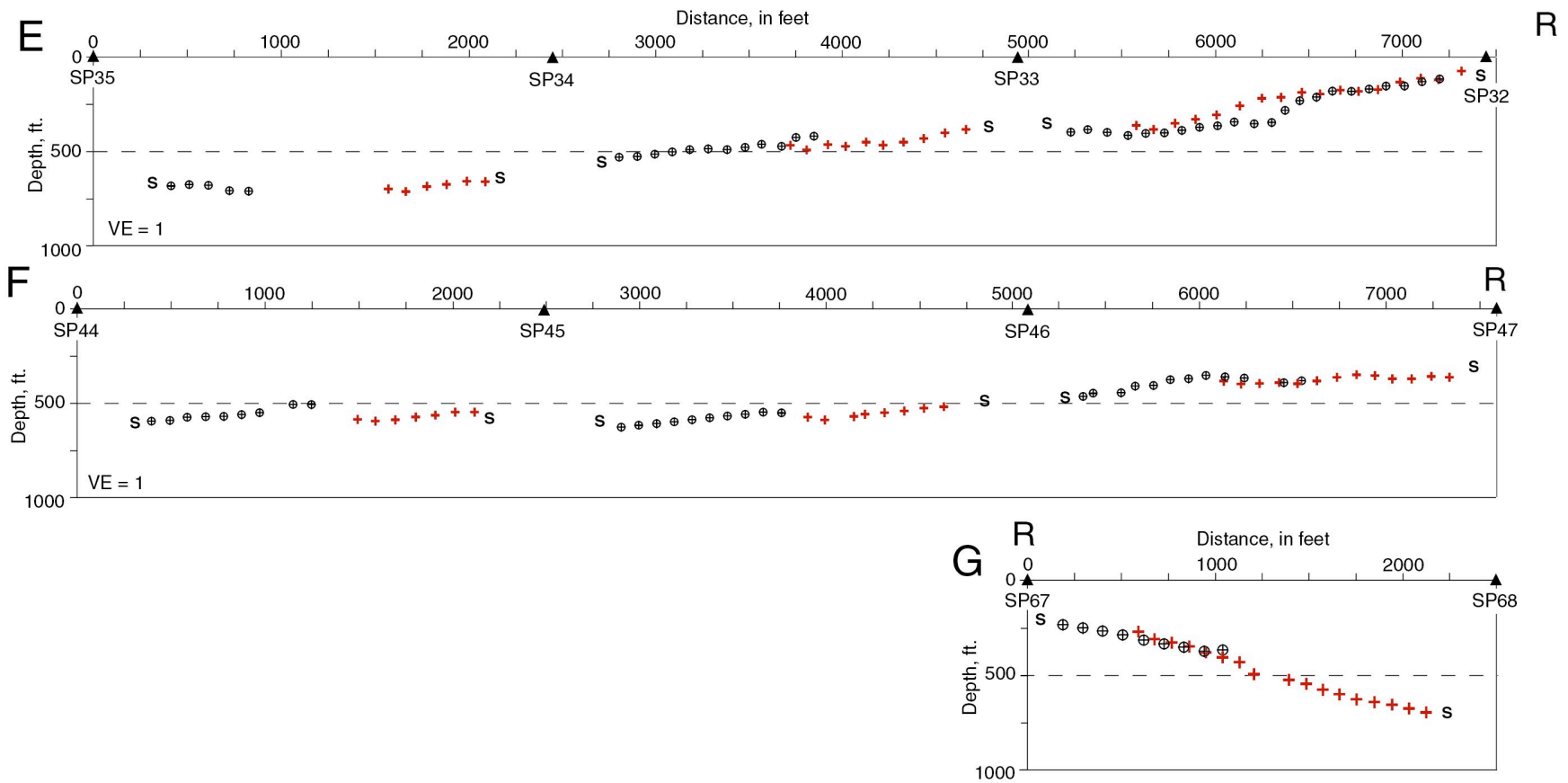
Figure 10 (page 3 of 3). [continued] He first defined the top of the intermediate layer and then combined layers 1 and 2 as an upper layer in a second two-layer problem to define the top of layer 3. R marks the approximate location of the crest of the Coyote Hills ridge in the profiles.
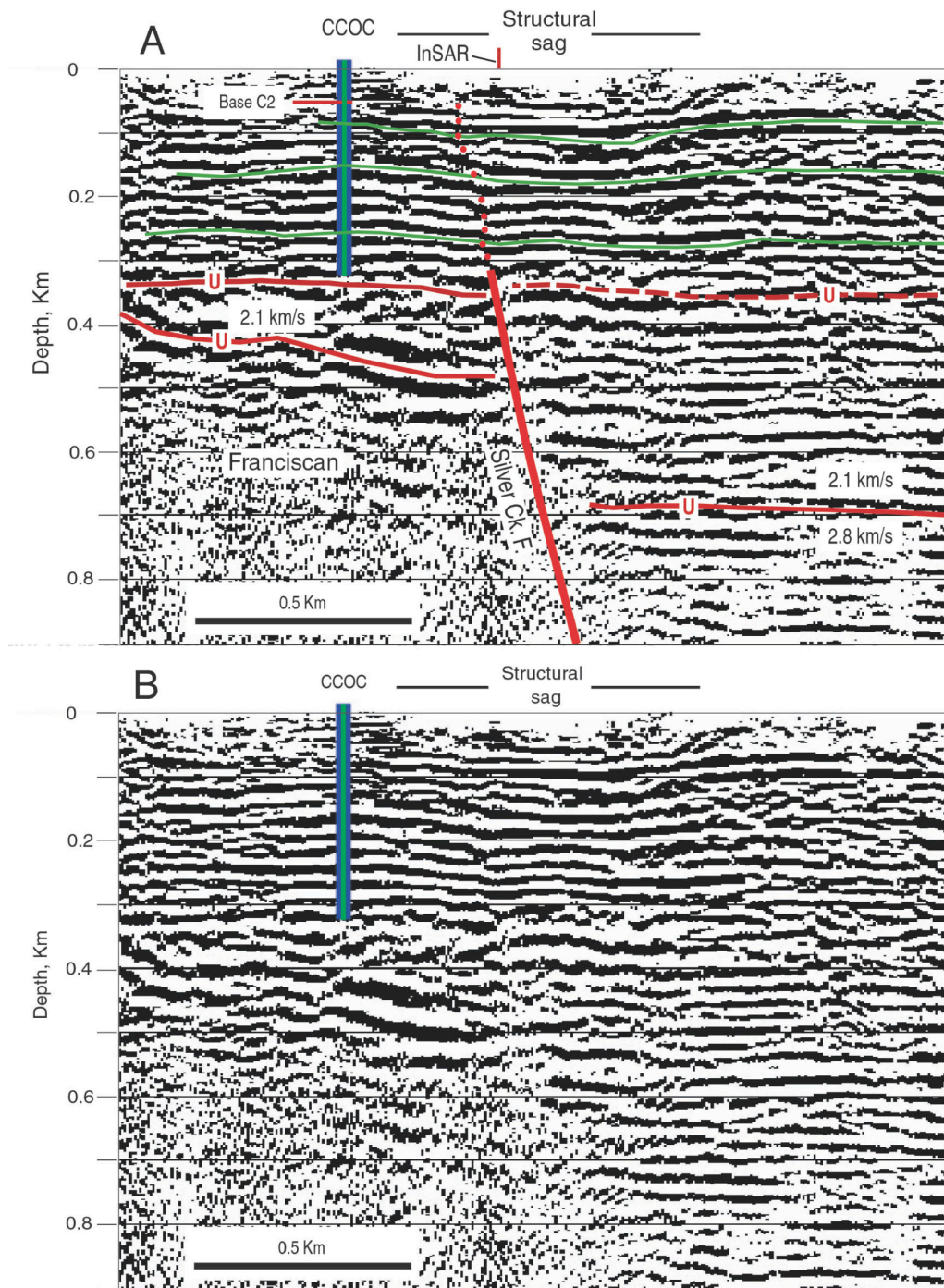
Figure 11. Detail of the minivibroseis seismic profile of figure 4 (unmigrated). A, interpretation showing the Silver Creek Fault and its bedrock tip, the negative flower structure overlying that tip, upward extension of the Silver Creek Fault (red dots), example correlated horizons (green), the approximate location of the InSAR boundary, vertical separation of 200 m on the 2.1 km/s base of the Quaternary section, unconformities (U), and the projected position of the base of sedimentary cycle 2 at the effective top of reflection imaging. B, the same profile without interpretation.
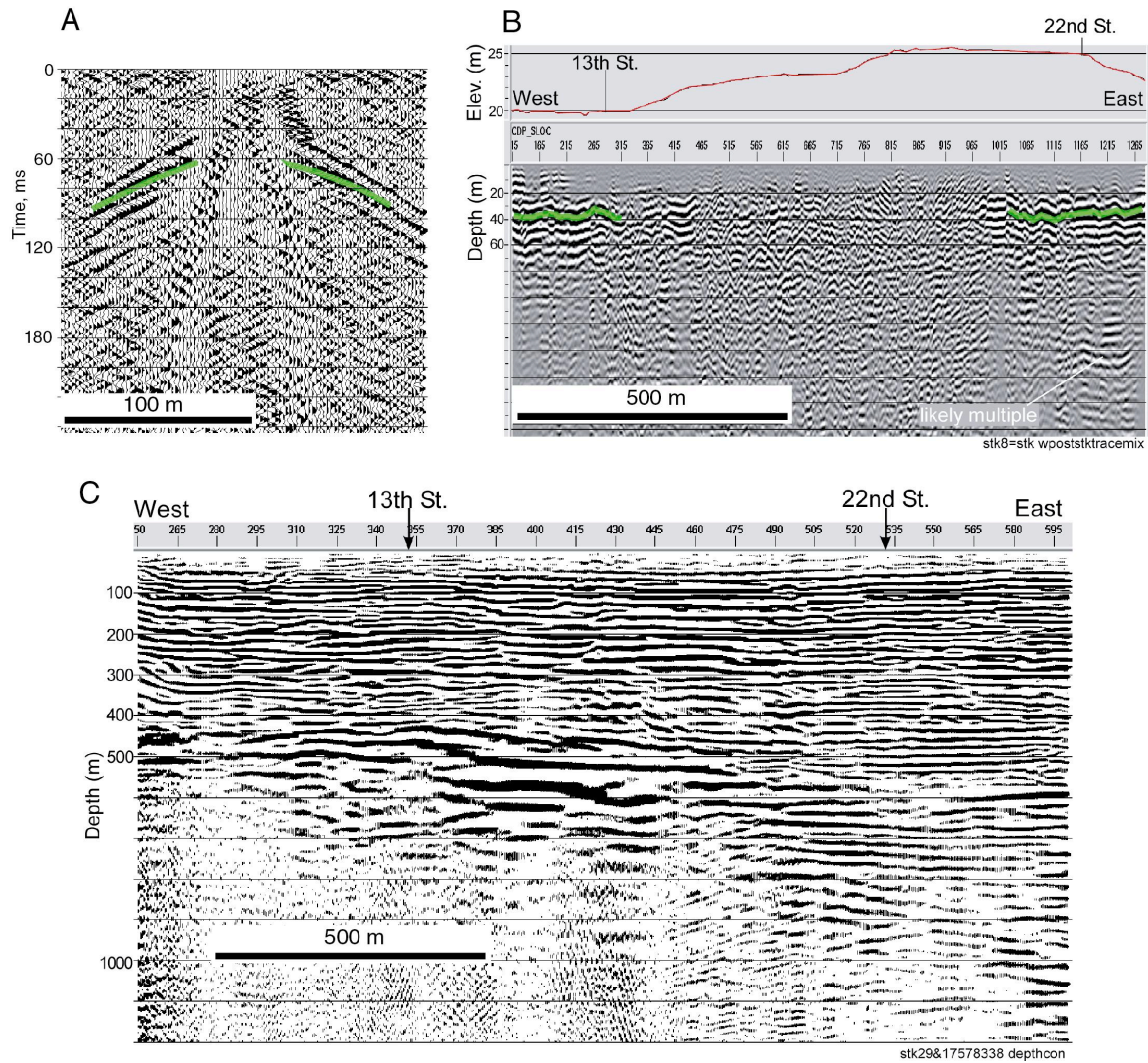
Figure 12. The Jackson Street hammer-source seismic reflection profile collected by R.A. Williams and others in 2007 across the structural sag. A CDP gather (*A*) from the east end, and the stacked profile (*B*) of the hammer profile show a distinct reflection that is highlighted in green. No interpretable reflection arrivals like this are recognized in the central part of the profile. The equivalent length of the 2002 minivibroseis line, C, (fig. 4) is shown for comparison (*C*). The hammer-source profile was collected along Jackson Street in San Jose, California, between 11th St and about 24th St.
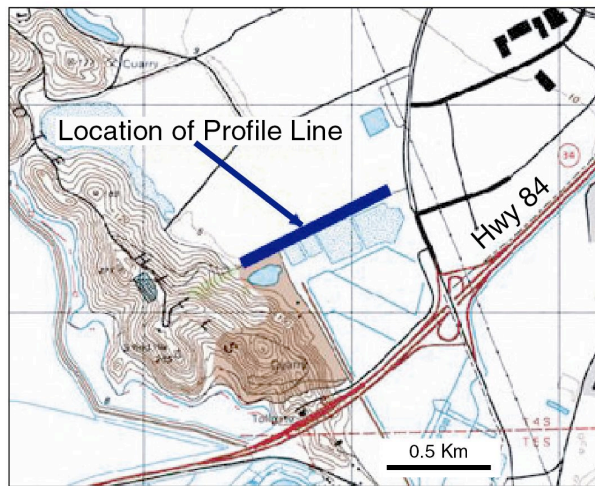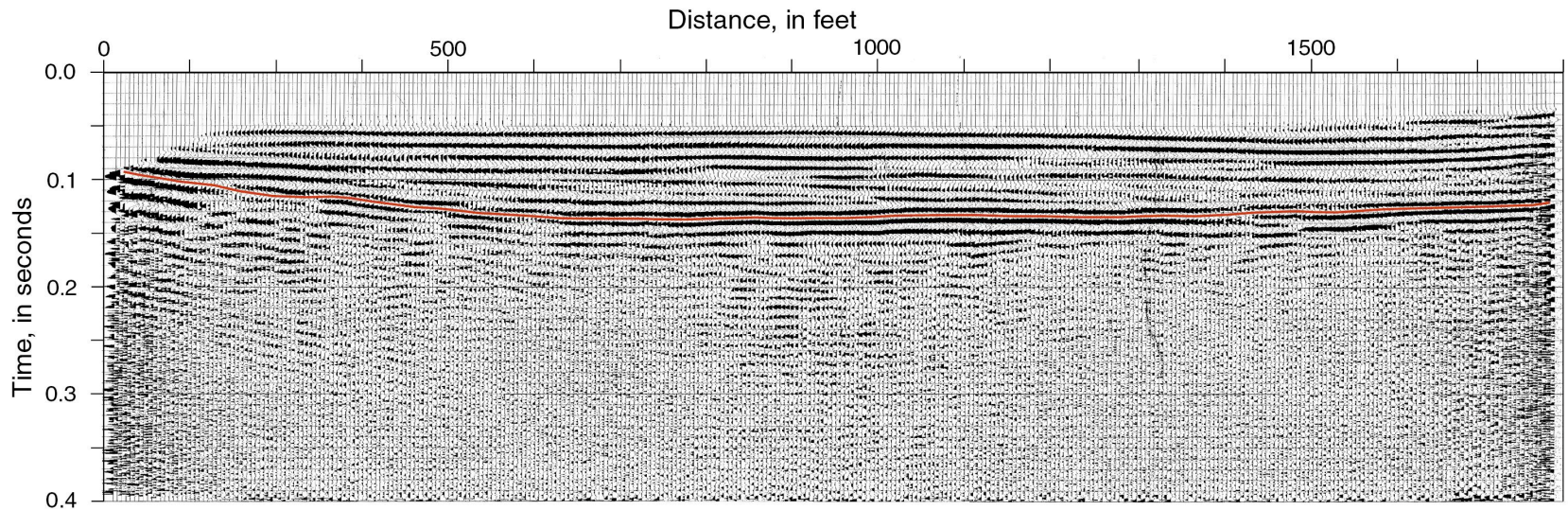
Figure 13. Seismic reflection profile just east of the Coyote Hills and north of Highway 84, California (see also fig. 8 for location). The top of Franciscan basement is highlighted in red. Line location and length are approximate. The profile was collected as an equipment test by R. Huggins and G. Church using a 16-lb hammer source and a 48 channel end-on array, 5-ft shot interval, 10-ft receiver interval, and a 50-ft near offset. Shown here with the kind permission of Geometrics.
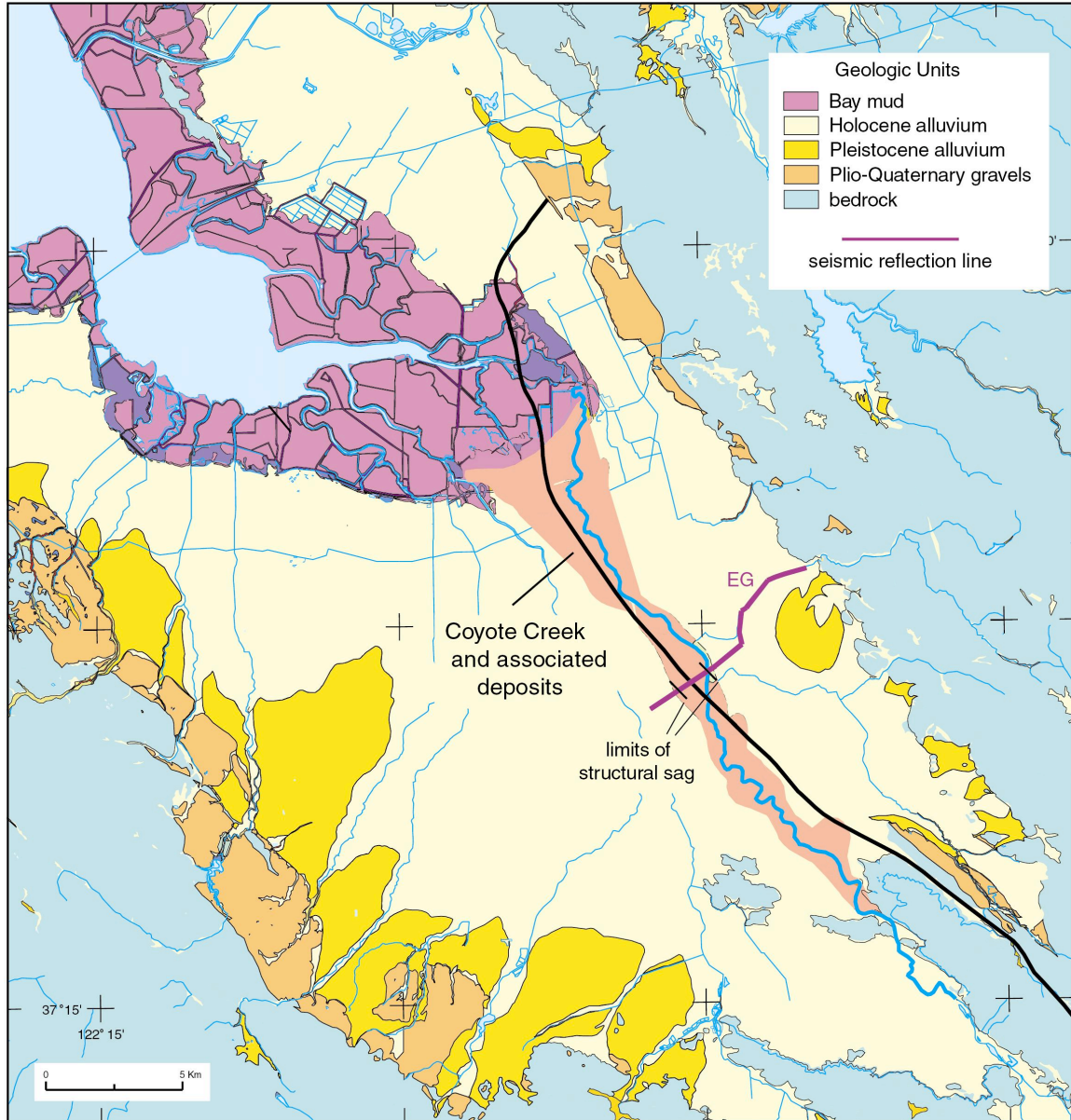
Figure 14. Map showing the spatial association of lower Coyote Creek and its associated deposits with the trace of the Silver Creek Fault, California, and the extent of the structural sag along the Evergreen seismic reflection profile (EG).
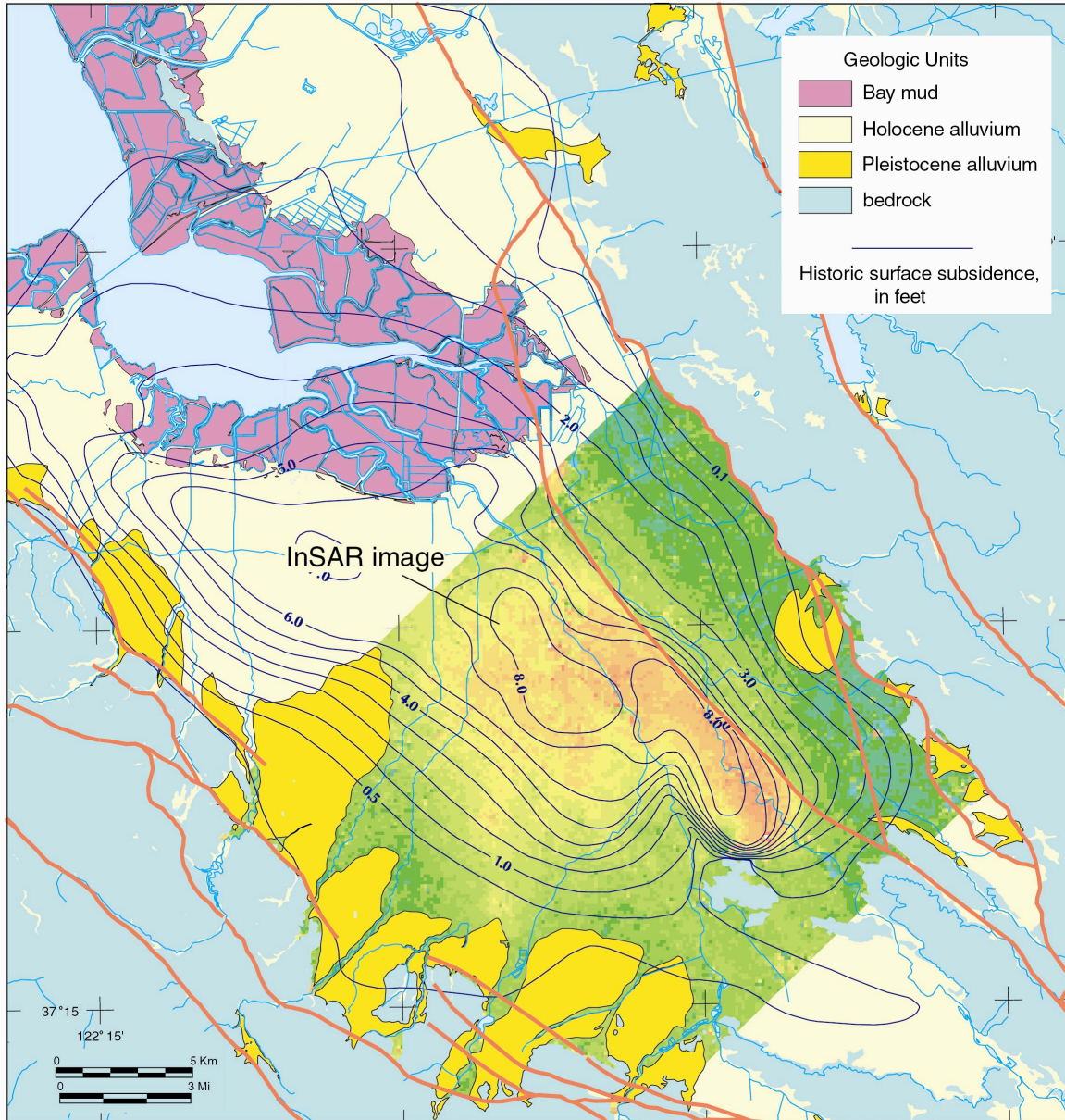
Figure 15. Historical surface subsidence due to groundwater withdrawal for the period 1934-1967 (Poland, 1971) in relation to the Silver Creek Fault, California. Subsidence contours based on an extensive network of survey level lines (Poland and Ireland, 1988, figs. 15 and 16). Modern recoverable annual subsidence is shown by an InSAR image (Galloway and others, 1999 and 2000) in which the bright colors represent surface elevation change of as much as about 2.5 cm.
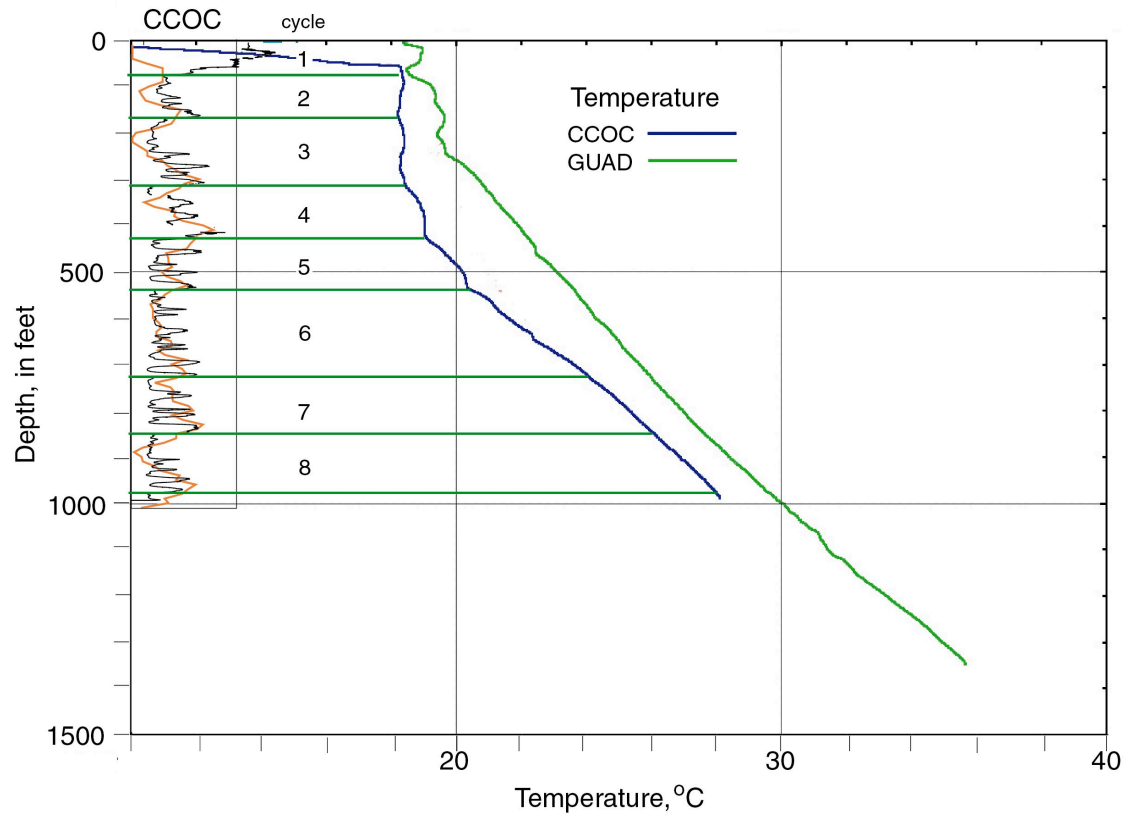
Figure 16. Temperature curves for wells CCOC and GUAD, Santa Clara Valley, California, showing perturbations in the smooth geothermal gradient. Stratigraphy and logs for well CCOC from figure 6. Temperature curves from C.F. Williams (Newhouse and others, 2004). The shallow steepening of the curves is due to the effect of long-term flow of ground water toward San Francisco Bay, whereas the local perturbations that correlate with the coarser parts of the sedimentary section result from ground-water movement due to pumping or other management practices (C.F. Williams, written commun., 2009; and see Williams and others, 1994).
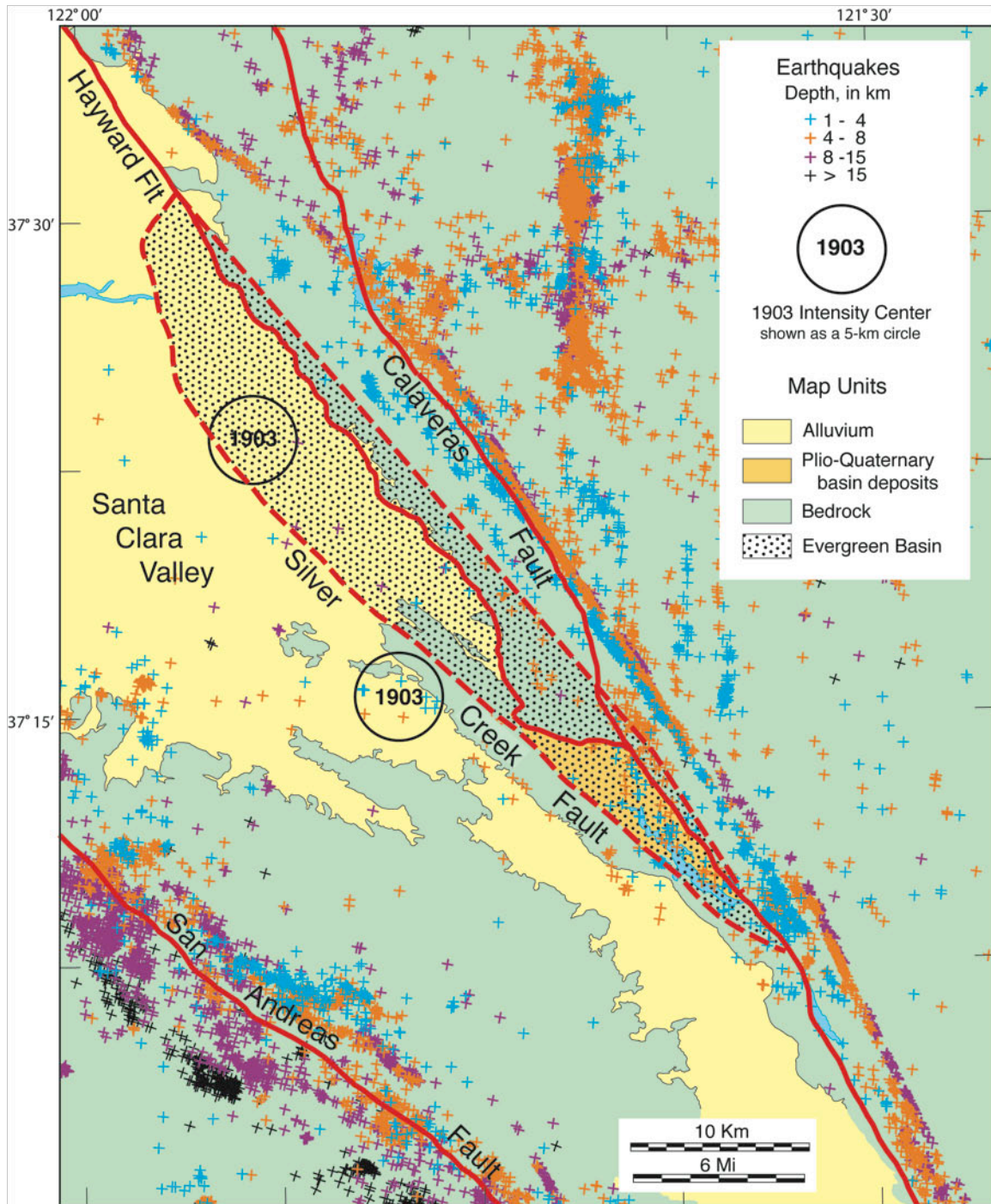
49

Figure 17. Map showing instrumental seismicity for the period 1984-2003 (double difference earthquakes of Waldhauser and Schaff, 2008), the Silver Creek Fault and Evergreen Basin, and the 1903 intensity centers of Bakun (1999 and 2008).